

## Magnetic classification of stony meteorites: 3. Achondrites

Pierre ROCHETTE<sup>1\*</sup>, Jérôme GATTACCECA<sup>1</sup>, Michèle BOUROT-DENISE<sup>2</sup>, Guy CONSOLMAGNO<sup>3</sup>,  
Luigi FOLCO<sup>4</sup>, Tomas KOHOUT<sup>5</sup>, Lauri PESONEN<sup>5</sup>, and Leonardo SAGNOTTI<sup>6</sup>

<sup>1</sup>CEREGE, CNRS Aix-Marseille University, BP80 13545 Aix en Provence, Cedex 4, France

<sup>2</sup>Museum National d'Histoire Naturelle, Paris, France

<sup>3</sup>Specola Vaticana, Vatican City State

<sup>4</sup>Museo Nazionale dell'Antartide, Università di Siena, Italy

<sup>5</sup>University of Helsinki, Finland

<sup>6</sup>Istituto Nazionale di Geofisica e Vulcanologia, Roma, Italy

\*Corresponding author. E-mail: [rochette@cerege.fr](mailto:rochette@cerege.fr)

(Received 09 January 2008; revision accepted 23 November 2008)

---

**Abstract**—A database of magnetic susceptibility measurements of stony achondrites (acapulcoite-lodranite clan, winonaites, ureilites, angrites, aubrites, brachinites, howardite-eucrite-diogenite (HED) clan, and Martian meteorites, except lunar meteorites) is presented and compared to our previous work on chondrites. This database provides an exhaustive study of the amount of iron-nickel magnetic phases (essentially metal and more rarely pyrrhotite and titanomagnetite) in these meteorites. Except for ureilites, achondrites appear much more heterogeneous than chondrites in metal content, both at the meteorite scale and at the parent body scale. We propose a model to explain the lack of or inefficient metal segregation in a low gravity context. The relationship between grain density and magnetic susceptibility is discussed. Saturation remanence appears quite weak in most metal-bearing achondrites (HED and aubrites) compared to Martian meteorites. Ureilites are a notable exception and can carry a strong remanence, similar to most chondrites.

---

### INTRODUCTION

Among stony meteorites, the ordinary chondrites (OC) group constitutes 90.3%, the other (i.e., non-ordinary) chondrites 5.8%, and the stony achondrites 3.9% (based on meteorite numbers in Grady [2000]). In two previous papers, we investigated systematically the magnetic properties of OC (Rochette et al. 2003) and non-OC (Rochette et al. 2008). This paper follows this scheme on stony achondrites. The magnetization ( $M$ ) of matter can be induced by an external field ( $H$ ) or be present in zero-field as remanent magnetization. The magnetic properties mostly discussed here will be magnetic susceptibility, i.e., the ratio  $M/H$  of induced magnetization to inducing field (of low intensity:  $<5$  mT) and the remanence measured after applying a “saturating” field (1 to 3 Teslas).

Low-field magnetic susceptibility ( $\chi$ ) has proved to be a rapid and non-destructive way to classify OC into the LL, L, and H classes, based on the distinct range of metal contents in each class (Rochette et al. 2003). Most non-OC groups also show a narrow range of  $\chi$  values, except C2, CM, and CV. Saturation remanence ( $M_{rs}$ ) was also compiled for chondrites to evaluate the range of likely remanent magnetization for

asteroids with chondritic compositions. Besides being a classification tool and a first step in more sophisticated magnetic applications (paleomagnetism: see Gattacceca and Rochette [2004]; magnetic anisotropy: see Gattacceca et al. [2005]; magnetic mineralogy: see Kohout et al. [2007]), both parameters have applications for the exploration of the solar system (e.g., Pesonen et al. 1993; Rochette et al. 2004). Therefore the same parameters have been analyzed in the different achondritic groups: the primitive (i.e., undepleted in metal) achondrites-acapulcoite-lodranite clan, winonaite, ureilite and differentiated ones—angrite, aubrite, brachinite, HED (howardite-eucrite-diogenite clan), and Martian meteorites. Lunar meteorites will be discussed in a separate paper devoted to a comparison with lunar samples from the Apollo and Luna missions (Rochette et al. 2008). Numerous magnetic studies have dealt with Martian meteorites (e.g., Cisowski 1986; Collinson 1986, 1997, and review in Rochette et al. 2005), as well as HEDs (Brecher et al. 1979; Nagata 1979; Nagata and Funaki 1984; Cisowski 1991; Morden 1992; Collison and Morden 1994; Gattacceca and Rochette 2004). The magnetic properties of other stony achondrite groups have received little attention, e.g., aubrites (Brecher et al. 1979; Gattacceca and Rochette 2004), ureilites

(Brecher and Furrman 1979), Angrites (Weiss et al. 2008), a mesosiderite (Collinson 1991), and a lunar meteorite (Nagata and Funaki 1986). On the other hand, lunar rocks have been extensively studied through the Apollo missions samples (see review in Fuller and Cisowski [1987]).

Rochette et al. (2001a) presented a common magnetic susceptibility database of the published data of Terho et al. (1991 and 1993) together with a number of new magnetic susceptibility measurements from the Vatican meteorite collection and the major collections from Italy (Table 1). Since then, the collections of natural history museums in Madrid and Paris and of the Ecole des Mines in Paris, have been measured and used in the Rochette et al. (2003) paper. After that publication, the new samples investigated have been in chronologic order, from the collections of Chicago (Field Museum), Albuquerque (IOM), London (NHM), Moscow (Vernadsky Institute), Rio de Janeiro (Museu Nacional), Tokyo (NIPR), Vienna (NHM), Houston (JSC), Washington (Smithsonian Institution), New York (AMNH), Zurich (ETH), Bern (NHM), Christchurch (Canterbury Museum), Los Angeles (UCLA), Lyon (ENSL), Tempe (ASU), Paris (UPMC), Berlin (Humboldt University), Edinburgh (National Museums Scotland), Cambridge (Harvard Mineralogical Museum), as well as various private collections. Furthermore, the Ottawa collection (Smith et al. 2006), the Berlin and four other European collections (Kohout et al. 2008), and the Shanghai Antarctic meteorite collection (Lin et al. 2008) have been investigated independently, and the data merged for this publication with the CEREGE database. While Ottawa and Moscow collections were investigated rather systematically, only a small selection of meteorites missing in the database were measured in the other collections (Table 1).

The total number of achondrite specimens currently in the database is 758; these are from 291 different meteorites, after tentative pairing of hot and cold desert ones. Total mass investigated is 28 kg. Table 1 summarizes the different collections used in the database and the instruments used for the magnetic susceptibility measurements. Although magnetic susceptibility data were collected by Terho et al. (1993) on iron and stony iron meteorites, we did not pursue this task as such meteorites pose a strong challenge in terms of measurement protocol (electrical conductivity effects, shape effects, saturation) with little potential reward. Based on magnetic susceptibility, it is practically impossible to distinguish between e.g., 80 and 100 wt% of metal, while it is very easy to distinguish between, e.g., 1 and 2 wt%.

### MAGNETIC MINERALOGY OF STONY ACHONDRITES

In stony achondrites, the abundances of the magnetic elements Fe and Ni vary according to geochemical class in the following wt% ranges, respectively: 20 and 1.2 in winonaites, 21–25 and 0.2–0.5 in brachinites, 19–44 and 1–1.8 in acapulcoites-Iodranites, 13–17 and 0.1–0.2 in ureilites, 11–15

and <0.04 for howardite-eucrite-diogenite (HED), 8–18 and <0.01 for angrites (Jarosewich 1990; Mittlefehldt et al. 1998). Other magnetic elements (mainly Co, Cr, and Mn) are usually present in negligible amounts, relative to Fe. Mn and Cr amounts are in the 0.2–0.5% range in angrites, HED and Martian samples.

The magnetic phases encountered in achondrites are essentially Fe-Ni alloys (e.g., Nagata 1979; Sugiura and Strangway 1987; Rubin 1997; Mittlefehldt et al. 1998). Metal is usually Ni poor, i.e., the kamacite phase. Minor taenite and tetrataenite are reported for HEDs, aubrites and lunar material. Minor schreibersite ((Fe,Ni)<sub>3</sub>P) and/or cohenite ((Fe,Ni)<sub>3</sub>C) are observed in aubrites, HEDs and ureilites (Mittlefehldt et al. 1998). Suessite ((Fe,Ni)<sub>3</sub>Si) has been described in ureilites (Keil et al. 1982; Herrin et al. 2007). Pyrrhotite (Kurat et al. 2004) and titanomagnetite (Floss et al. 2003) coexist with metal in angrites and in Martian meteorites magnetization is carried by magnetite and pyrrhotite (Rochette et al. 2005). Note that shock induced production of metallic nanoparticles has been observed in the olivine of four Martian meteorites: the chassignite Northwest Africa (NWA) 2737 and three lherzolithic shergottites (Van de Moortele et al. 2007; Hoffmann et al. 2008). Several Fe-bearing phases including metal, magnetite, cohenite, schreibersite, and suessite yield similar apparent volumic susceptibility of 3 SI for a multidomain sphere. Therefore, depending on density, the specific susceptibility varies in the 400–600 × 10<sup>-6</sup> m<sup>3</sup>/kg range. In the case of ferromagnetic pyrrhotite, depending on grain size, specific susceptibility varies in the 10–60 × 10<sup>-6</sup> m<sup>3</sup>/kg range (Dekkers 1988). A correlation between susceptibility and metal amount was demonstrated for OCs in Rochette et al. (2003), although dispersion may arise in meteorites that contain abundant tetrataenite. For magnetite-bearing carbonaceous chondrites such a correlation was described in Rochette et al. (2008). The correlation between susceptibility and metal content has been calibrated experimentally by measuring dispersed synthetic spherical grains in plaster with variable dilution. These grains have on average a diameter of 5 μm (see their description in Chevrier et al. 2006) and are therefore in a multidomain state: the threshold to the stable single domain state is below 0.1 μm. Figure 1 shows a perfect linear correlation with metal content from 0.1 to 50%, leading to an apparent specific susceptibility of 544 × 10<sup>-6</sup> m<sup>3</sup>/kg for the metal spheres used. However, a higher susceptibility can be obtained if the grains are anisometric. For example for randomly oriented prolate grains with an axial ratio of 2 (or 0.4 for oblate grains), the mean susceptibility is 1.25 times higher (Rochette et al. 2003). Interaction between particles and imperfect dispersion of the metal can also lead to higher susceptibility: for example, a hollow sphere may have the same apparent volume susceptibility as a solid sphere. A realistic equivalent of the hollow sphere case might be a meteorite with a perfectly connected dense network of metal veins, as is the case in mesosiderites. We therefore predict that mesosiderites (with about 50% of metal) have the same

Table 1. List of meteorite collections entered in the database (in chronological order of measurements, and with the same numbering as in Rochette et al. 2003), as well as number of measured specimens and the measurement instruments used. 1–5, 6–7, 17, 22, 31, and 33 were previously and partly published in Rochette et al. (2001a), Thero et al. (1993), Smith et al. (2006), Kohout et al. (2008), and Lin et al. (2008). For 22 the different collections included (number of samples within brackets) are the Swedish Museum of Natural History, Stockholm (1), University of Oslö (1), Tartu University (1), Geology and Mineralogy Museum, Vilnius (1), Geological Survey of Estonia, Tallin (1), Chemical University, Prague (1).

#	N	Collection	Instruments
1	19	Vatican Observatory, Castel Gandolfo	KLY-2
2	4	University La Sapienza, Roma	KLY-2
3	34	Museo Nazionale dell'Antartide, Siena	KLY-2, MS2B
4	5	San Giovanni in Persiceto	KLY-2
5	39	Private collections	KLY-2, MS2B, SM30
6	5	Prague Museum	KLY-2
7	37	Helsinki database (1993)	KLY-2, RISTO 5
8	127	Natural History Museum, Paris	KLY-2, MS2B, SM30
9	8	Natural History Museum, Madrid	KLY-2
10	7	Mines School Museum, Paris	MS2B, SM30
11	80	Vernadsky Institute Moscow	MS2B, SM30, KLY-2, IMVO
12	23	Natural History Museum London	MS2B, SM30
13	3	Field Museum, Chicago	SM30
14	4	NIPR, Tokyo	KLY-2
15	9	IOM University of Albuquerque	MS2B, SM30
16	15	Natural History Museum, Vienna	MS2B, SM30
17	76	Geological Survey, Ottawa	SI-2B
18	25	Museu Nacional, Rio de Janeiro	MS2B, SM30
19	61	Johnson Space Center, Houston	MS2B, SM30
20	66	Smithsonian Institution, Washington, D.C.	MS2B, SM30
21	29	Natural History Museum, New York	MS2B, SM30
22	6	Helsinki database (2008)	TH1
23	4	Natural History Museum, Bern	MS2B, SM30
24	2	ETH, Zürich	MS2B, SM30
25	4	Canterbury Museum, Christchurch	SM30
26	6	UCLA, Los Angeles	MS2B, SM30
27	11	ENS, Lyon	MS2B, SM30
29	5	ASU, Tempe	MS2B, SM30
30	15	UPMC, Paris	MS2B, SM30
31	11	Humboldt University Berlin	TH1, MS2B, SM30
32	7	National Museum, Edinburgh	MS2B, SM30
33	9	Polar Research Institute, Shanghai	MS2B
34	2	Harvard Mineralogical Museum, Cambridge	MS2B

susceptibility as pure metallic meteorites. But the strongest effect is observed for superparamagnetic metal grains (grain size below 20 nm at room temperature); in that case, susceptibility can be up to 10 times higher than the multidomain value (see Fuller and Cisowski 1987; Van de Moortele et al. 2007). For all these reasons, the correlation between metal (plus carbide, phosphide, etc.) content and magnetic susceptibility is not completely straightforward and magnetic susceptibility provides an upper limit on the metal content in a meteorite.

For comparison, the other Fe- or Ni-bearing phases, paramagnetic silicates (olivine, pyroxene) or oxides (chromite, ilmenite, spinel) and antiferromagnetic troilite have no remanence and comparatively very low susceptibility at room temperature. The most Fe-rich minerals of this kind, fayalite and troilite, yield susceptibility values of 1.2 and 0.2–

$0.4 \times 10^{-6} \text{ m}^3/\text{kg}$ , respectively (Carmichael 1989; Coey et al. 1976; Kohout et al. 2007). In the case of negligible amounts of a strongly magnetic phase, and assuming all iron is in the  $2^+$  non interacting paramagnetic state, one can predict that  $\chi = F \times 25.2 \cdot 10^{-9} \text{ m}^3/\text{kg}$ , where F is the weight % of Fe, neglecting the other magnetic elements such as Ni, Cr, Co or Mn (Rochette 1987). Therefore, the maximum paramagnetic susceptibility of achondrites (taking an Fe wt% range of 8 to 25) should vary from 200 to  $625 \cdot 10^{-9} \text{ m}^3/\text{kg}$  (i.e.,  $\log \chi$  in the 2.3–2.8 range).

## MEASUREMENT AND DATABASE CONSTRUCTION

Measurement procedures have been discussed in detail in Rochette et al. (2001a, 2003, 2008) and will only be summarized here. A large coil (8 cm) alternating field bridge KLY-2 (manufactured by AGICO, or its custom-made

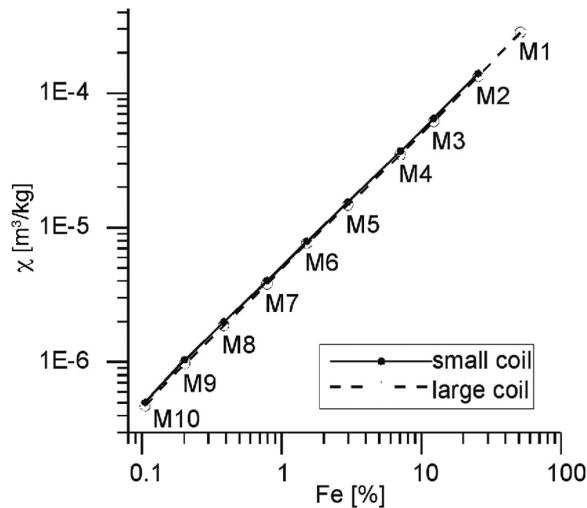


Fig. 1. Susceptibility  $\chi$  as a function of metal amount (in wt%) for a synthetic dispersion of 5  $\mu\text{m}$  metallic iron spheres into plaster. The samples with different metal amount (M1 to M10) were measured using both the large and small coils of KLY-2.

equivalent, for the Helsinki data) was used, allowing samples up to a mass of 450 g to be measured, although coil saturation may be already reached for 50–100 g highly magnetic samples. The high homogeneity of the solenoid coil internal field allowed us to obtain reliable results on samples with anisometric shape (fragments, slice, full stones). For each measured specimen, the decimal logarithm of apparent mass specific susceptibility  $\chi$  is tabulated (in  $10^{-9} \text{ m}^3/\text{kg}$ ). The use of log units is justified for presentation reasons (as the data vary by 3 orders of magnitude) and also by the fact that  $\chi$  is expected to follow a log normal distribution for a given formation or parent body (Latham et al. 1989). Therefore, it is more representative to average the data in terms of  $\log\chi$  rather than  $\chi$ . We selected specimens with a minimum mass of 3 g (i.e., about one cubic centimeter). Smaller masses were measured only in the case of rare meteorites for which no larger specimens were available. In any event, the precision remained better than 0.01 (in  $\log\chi$ ). As the KLY-2 is quite awkward to transport, for a number of collections we used a more portable coil system, the MS2B instrument (manufactured by Bartington). This instrument is less precise than the KLY-2 but reasonably well cross-calibrated with the KLY-2 (Sagnotti et al. 2003). The Ottawa collection has been measured using a SI-2B bridge (from Sapphire; Smith et al. 2006). Cross calibration with the KLY-2 is not specifically provided, but correlating the measurements from the CEREGE and Canadian databases on the same meteorite (Smith et al. 2006) show a good one to one correspondence. Therefore the Canadian data were merged into our database without any correction. Cross-calibration with the Helsinki (1993) data was discussed in Rochette et al. (2003). For the Helsinki (2008) database Kohout et al. (2008) used a portable instrument (Hämäläinen TH-1) of low sensitivity compared

with the KLY-2. Therefore we merged in our database only the data with sufficient accuracy (i.e., large enough mass and  $\log\chi$ ). Smith et al. (2006) reported a noticeable frequency dependence of  $\chi$  for some meteorites. Therefore we choose to use data obtained at the lowest frequencies: 900, 1000, 815 Hz for the KLY-2, MS2B and SI-2B instruments, respectively. Finally, new measurements performed in Moscow were obtained using a large coil bridge IMVO (manufactured by Geologorazvedka), which was cross-calibrated on site with a KLY-2.

For samples that would not fit into the KLY-2, IMVO or MS2B coils we used another instrument: the SM30 (manufactured by ZH instruments) or its older version, KT5. The instrument is an LC oscillator that uses a flat coil placed next to the surface of the sample to be measured. Due to the highly variable magnetic field created at the coil front, the output critically depends on the shape of the sample, especially its surface facing the instrument; the optimal configuration is a flat cut surface. About 99% of the signal comes from a cylinder of 8 cm in diameter extending outwards 5 cm from the coil front; volume susceptibility can be directly output for an end-cut stone larger than this volume. Cross-calibration of the KT5 or SM30 with the KLY-2 instrument is described by Lecoanet et al. (1999) and Gattacceca et al. (2004a). For a slice of constant thickness less than 5 cm, a known correction factor can be applied. In addition, Gattacceca et al. (2004a) provide a calibration curve for correcting SM30 measurements on uneven shaped samples such as full stones or fragments. This procedure has been further demonstrated in Folco et al. (2006). In order to obtain mass specific values from SM30 measurements, the output has to be divided by density (for the same meteorite, if available, or else from its type average), as obtained from the Terho et al. (1991) and Britt and Consolmagno (2003) databases. Gattacceca et al. (2004a) have shown that there is good agreement between the SM30 and KLY-2 measurements for a wide range of meteorites.

The various sources of error in low field susceptibility measurements of meteorite specimens have been detailed by Terho et al. (1993) and Rochette et al. (2001a). The effect of a fusion crust has been shown to be negligible for pieces larger than  $1 \text{ cm}^3$  with  $\log\chi$  greater than 3.5. The anisotropy of the magnetic susceptibility (AMS), due either to a preferred orientation of magnetic grains or to the shape of the sample, is a more serious problem. Tests and models have shown that the error in mean  $\log\chi$  due to anisotropy can reach  $\pm 0.1$  when only one arbitrary direction is measured. Therefore, whenever it was possible,  $\chi$  was averaged from measurements taken along three perpendicular directions. Gattacceca et al. (2005, 2008) provide a database of the anisotropy ratio observed in some achondrites. It is less than 1.1 for Martian meteorites, but can peak at 1.8 for HED samples. Shape effect becomes marginal for  $\log\chi \leq 4.9$ , i.e., for all groups except acapulcoites/lodranites and winonaites.

Our database has one entry per specimen, except for the Terho et al. (1991, 1993) data where the average per meteorite was used and lists the mass of the specimen (or group of specimens),  $\log\chi$  and the collection provenance. Only the average of data for each meteorite is shown in Table 2 and 3. In the average of samples from the same meteorite (the arithmetic mean of  $\log\chi$  in agreement with the log normal distribution invoked above), equal weight has been given to each entry with a mass larger than 3 g. In a case of three entries with, for example, masses of 1, 20, and 30 g, only the latter two were used. On the other hand we use several samples of less than three grams to derive the mean when large samples were unavailable. Outliers are defined by difference with the mean exceeding 3 standard deviation (s.d.); such outliers (4 specimens) are not used to compute the mean value at the meteorite level. Typically, the s.d. for a given chondrite is less than 0.1 (on average 0.07 see Rochette et al. 2003 and 2008). Larger s.d. was observed only when shape anisotropy was important ( $\log\chi > 5$  as in CR, CH, E) or in the case of variable terrestrial weathering. Apart from ureilites, achondrites show a s.d. for a given meteorite significantly larger than that seen for chondrites (on average about 0.15, see Table 4). This indicates that achondrites are more heterogeneous (in terms of magnetic mineral distribution) than chondrites, thus implying that classifying these samples by their magnetic properties will be less robust. One may wonder if the specimen size does control mean s.d. and if the higher dispersion in achondrites could be linked to on average smaller masses measured on those rare meteorites. Median masses computed in Table 4 indicate that this is not the case. The more or less pronounced heterogeneity of the different achondrite groups will be further discussed in the following sections. Figure 2 (after Table 4) presents the average  $\log\chi$  for each class investigated, compared to some chondrite groups. The spread of  $\log\chi$  values within a group is usually larger for achondrites than for chondrites. In Figure 2 one clearly sees the dichotomy between the metal-rich primitive achondrites ( $\log\chi > 4$ ) and the other metal-depleted groups ( $\log\chi < 4$ ), although some overlap exists for aubrites and brachinites. Suspected pairs among the Sahara, Omani, or Antarctic finds are counted as a single entry for such means. This pairing, based on geographical proximity, similar petrography and  $\log\chi$  values, was necessary to avoid overweighting of the group means by Antarctic and hot desert samples.

## THE MAGNETIC SUSCEPTIBILITY OF ACHONDRITES

### Ureilites

The three measured ureilite falls (Dyalpur, Haverö, Novo Urei) yield a well-grouped mean at  $4.95 \pm 0.14$ . The two lowest  $\log\chi$  (near 3.6) values are found in two Antarctic ureilites reported as anomalous, Elephant moraine (EET)

83309-87720 and Meteorite Hills (MET) 01085, the latter being devoid of olivine. The whole group shows a lower average value ( $4.39 \pm 0.31$ , excluding the two above-mentioned outliers) that could be attributed to weathering of metal in the finds (50 out of 53 meteorites). However, weathering cannot account for the whole dispersion: for example the Antarctic Frontier Mountain (FRO) ureilite impact melt breccia (FRO 9036 paired family) which shows a very low weathering grade (W1) has one of the lowest  $\log\chi$  ( $3.95 \pm 0.2$ ) in ureilites. Note that for the FRO ureilites we followed Welten et al. (2006) in distinguishing 3 different falls among them. On the other hand, two finds show very high  $\log\chi$ : Goalpara and Dar al Gani (DaG) 692 at 5.23 and 5.32, respectively. Both are highly shocked, and DaG 692 is a breccia. We note that DaG 692 is clearly distinct from the other DaG ureilites, at  $4.32 \pm 0.18$ .

A better representation of the effect of brecciation and shock (after Goodrich 1992 and Mittlefeldt et al. 1998) can be found on the histogram of Fig. 3: the lowest and highest  $\log\chi$  values correspond to either brecciated or highly shocked ureilites (like the falls Dyalpur and Haverö). Brecciation is also responsible for a larger individual s.d.: 0.17 on average, compared to the average individual s.d. for unbrecciated ureilites of 0.06 (Table 4). Assuming that shock and brecciation have altered the primary metal amount in the ureilite parent body, a more representative average could be obtained by selecting only the unbrecciated low- to medium-shocked ureilites:  $4.34 \pm 0.23$  (including the two falls Dyalpur and Novo Urei). However, this mean value is clearly biased by weathering, as Dyalpur and Novo Urei show the highest values in that population. No correlation is found between the Fa (mol%) value of olivine cores and metal amount (Fig. 4). This is in favor of the idea of Warren and Huber (2006) that metal production by olivine reduction is restricted to the rim of the olivine crystals and cannot account for the core Fa (mol%) range observed in ureilites.

It is worth pointing out a distinct behavior of Antarctic ureilites. Among all ureilites, the seven meteorites with  $\log\chi < 4$  are from six different ice fields in Antarctica. Among the unbrecciated low to medium shock level, all ureilites with  $\log\chi \leq 4.2$  (12 meteorites) are from Antarctica, except Nova 1. They again come from six different ice fields (Allan Hills, Elephant Moraine, Frontier Mountain, Grove Mountains, Lewis Cliff, Queen Alexandra Range), thus excluding further pairing. On the other hand, among the remaining 26 meteorite finds with the same petrology with  $\log\chi \geq 4.28$ , only 9 are from Antarctica, the rest being from hot deserts. Metal weathering cannot account for the distinctly lower metal content of Antarctic ureilites, as the hot desert ureilites are often quite weathered too. Therefore, we put forward the working hypothesis that the provenance of ureilites in terms of parent body has changed through time toward a more metal-rich petrology, as on average terrestrial ages for Antarctic finds are much older than for hot deserts

Table 2. Decimal  $\log\chi$  (in  $10^{-9}$  m<sup>3</sup>/kg) for achondrites except HEDs, after tentative pairing for desert finds. For ureilites, the anomalous (an), brecciated (br), or unbrecciated and highly shocked (h) characters are indicated. Among SNC meteorites the two magnetic subgroups are separated. Arithmetic mean and standard deviation (s.d., computed using N-1 as normalizer) of  $\log\chi$  are provided when more than one specimen was measured. N: number of specimens used in the mean (in brackets number of outliers); m: cumulate mass measured. Provenance code: see # in Table 1. Anomalies not included in Table 4 means are listed at the end for each group (name in italics). Pairing notes: (1) DaG 084, 164, 165, 319, 340, 485, 494, 660, 897 (2) FRO 90036-54-168-228-233, 93008, 95028, 01012, 03022.

Meteorite	Group	$\log\chi$	s.d.	N	m (g)	Provenance
Angra dos Reis	ANG	2.61	0.15	4	82	1, 8, 18
D'Orbigny	ANG	3.11	0.16	3	5.8	5, 15, 27
LEW 86010-87051	ANG	2.62	0.07	3	2.1	19
NWA 1296	ANG	2.92	0.08	2	751.7	5, 30
NWA 1670	ANG	2.98	0.02	2	14.6	5, 27
NWA 4590	ANG	2.82		1	28.3	5
NWA 4801	ANG	3.14		1	0.2	27
NWA 5376	ANG	2.84		1	1.5	31
Sahara 99555	ANG	2.93		1	8.2	11
<i>NWA 3164-5167</i>	ANG	4.54		1	2.3	5, 30
ALH 84007-12	AUB	4.15	0.27	2	9.3	19, 20
Aubres	AUB	3.91	0.35	5	49.6	8, 11, 29, 31
Bishopville	AUB	3.41	0.56	9	87.8	1, 2, 7, 8, 10, 17
Bustee	AUB	4.21	0.70	3	19.4	8
Cumberland Falls	AUB	4.17	0.52	7	429.1	1, 7, 8, 9, 11, 17, 22
Khor Temiki	AUB	2.84	0.40	3	10.7	4, 8, 17
LAP 03719	AUB	1.96		1	16.8	19
LAR 04316	AUB	3.61		1	3.2	19
Mayo Belwa	AUB	3.67	0.03	4	209.1	8, 11, 17
Mt. Egerton	AUB	4.57	0.70	9	419	8, 20, 25, 31
Norton County	AUB	3.51	0.29	8	526	4, 7, 11, 17, 18, 32
NWA 4420	AUB	4.21	0.45	2	589.7	30
Peña Blanca	AUB	2.92	0.42	5	53.9	1, 4, 11, 17
Pesyanoë	AUB	3.68	0.30	4	207.8	8, 11, 17
QUE 97289	AUB	4.88		1	10.7	19
Shallowater	AUB	4.88	0.01	2	21.1	7, 8
ALH 84025	BRA	4.27		1	0.8	19
Brachina	BRA	3.97	0.42	4	26.1	12, 20
Eagles Nest	BRA	3.41	0.06	2	16.4	17, 21
EET 99402-7	BRA	2.95	0.05	3	57.2	19
Hughes 26	BRA	3.97		1	46	5
LEW 88763	BRA	3.73		1	0.3	19
Nova 3	BRA	4.15		1	15	11
NWA 3151	BRA	3.35		1	100	5
Reid 13	BRA	3.96	0.08	3	10.9	5, 15, 24
ALHA75005	SNC	3.38		1	0.24	19
Dho 378	SNC	3.40		1	0.5	11
Governador Valadares	SNC	3.30	0.07	3	3.4	8, 18
GRV 020090	SNC	3.14		1	7.5	33
Lafayette	SNC	3.36	0.08	3	30.5	12, 21
Los Angeles	SNC	3.42	0.05	3	14.4	1, 8, 21
MIL 03346	SNC	3.67		1	25	20
Nakhla	SNC	3.21	0.08	7	312	1, 6, 8, 11, 17, 21, 32
NWA 1669	SNC	3.20		1	0.2	5
NWA 1950	SNC	3.76		1	1.7	5
NWA 817	SNC	3.82		1	2.4	27
NWA 998	SNC	3.60	0.04	2	1.8	5
ALH 84001	SNC	2.81		1	0.4	19
Chassigny	SNC	3.15	0.23	2	37.2	1, 7, 11

Table 2. *Continued.* Decimal  $\log\chi$  (in  $10^{-9}$  m<sup>3</sup>/kg) for achondrites except HEDs, after tentative pairing for desert finds. For ureilites, the anomalous (an), brecciated (br), or unbrecciated and highly shocked (h) characters are indicated. Among SNC meteorites the two magnetic subgroups are separated. Arithmetic mean and standard deviation (s.d., computed using N-1 as normalizer) of  $\log\chi$  are provided when more than one specimen was measured. N: number of specimens used in the mean (in brackets number of outliers); m: cumulate mass measured. Provenance code: see # in Table 1. Anomalies not included in Table 4 means are listed at the end for each group (name in italics). Pairing notes: (1) DaG 084, 164, 165, 319, 340, 485, 494, 660, 897 (2) FRO 90036-54-168-228-233, 93008, 95028, 01012, 03022.

Meteorite	Group	Log $\chi$	s.d.	N	m (g)	Provenance
DaG 476-489-1037	SNC	2.81	0.15	6	90.5	3, 8, 11, 17, 18
Dho 19	SNC	2.84	0.07	3	2	5, 11
EETA79001	SNC	2.84	0.05	3	2.9	7, 19
LAR 06319	SNC	3.28		1	35.6	19
NWA 1068	SNC	3.20	0.08	4	10.1	5, 18
NWA 1195	SNC	3.12		1	0.7	5
NWA 4468	SNC	2.78		1	34	5
NWA 4783	SNC	3.02		1	14.7	30
NWA 4925	SNC	2.82		1	19.2	31
NWA 856	SNC	2.95	0.03	2	8.3	5
QUE 94201	SNC	3.11		1	0.3	19
SAU 005-60-90-94	SNC	2.86	0.11	4	25.1	1, 8, 11, 23
Shergotty	SNC	3.15	0.15	3	82.4	8, 11, 17
Zagami	SNC	2.79	0.15	7	178.9	7, 8, 11, 17, 18, 21
<i>NWA 2737</i>	SNC	4.41		1	0.8	5
Acfér 277	URE	4.53		1	7.8	16
Acfér 360	URE	4.33		1	60	5
ALHA77257	URE	4.57		1	117.3	20
ALHA78019	URE	4.18		1	0.4	19
ALH 81101	URE h	4.68		1	2.8	19
ALH 84136	URE	4.19		1	7.6	19
CMS 04044-48	URE	4.47	0.02	2	15.7	19
DaG 692	URE br	5.32		1	43	3
DaG 340 (1)	URE br	4.32	0.18	11	106.8	3, 16, 21, 23
Dho 295	URE	4.40		1	12.5	11
Dho 132	URE	4.43		1	0.96	5
Dingo Pup Donga	URE	4.40	0.00	2	6.3	12, 20
Dyalpur	URE h	4.90	0.08	2	20.3	8, 11
EET 83225-87511	URE	3.84	0.07	2	12.	19
EET 90019	URE	4.13		1	10.2	19
EET 96042	URE	4.01		1	10.2	19
El Gouanem	URE	4.38		1	3.1	8
FRO 90036 (2)	URE br	3.94	0.21	8	75.5	3
FRO 97013	URE	4.08		1	20.1	3
FRO 01030	URE	3.93		1	3.5	3
GRA 95205-98032	URE h	4.37	0.09	2	838	19
GRV 021729	URE	4.07		1	3	33
GRV 021512	URE	3.97		1	143	33
GRV 052382	URE	4.51		1	1.9	33
Goalpara	URE h	5.22	0.04	2	58	8, 11
HaH 126	URE	4.56		1	21.2	31
Hajma A	URE h	4.19	0.10	2	599.8	12, 13
Haverö	URE h	5.13	0.03	3	18.7	7, 11, 17
Hughes 007	URE	4.33	0.06	3	3.1	17, 21, 23
Hughes 009	URE	4.28	0.08	3	8.5	17, 21, 23
Kenna	URE	4.53	0.08	7	187.8	8, 17, 31
LAP 02382	URE	4.35		1	37.6	19
LAP 03587	URE	4.54		1	87	19
LAR 04315	URE	4.50		1	1008	19
LEW 85328	URE	4.20		1	19	19

Table 2. *Continued.* Decimal  $\log\chi$  (in  $10^{-9}$  m<sup>3</sup>/kg) for achondrites except HEDs, after tentative pairing for desert finds. For ureilites, the anomalous (an), brecciated (br), or unbrecciated and highly shocked (h) characters are indicated. Among SNC meteorites the two magnetic subgroups are separated. Arithmetic mean and standard deviation (s.d., computed using N-1 as normalizer) of  $\log\chi$  are provided when more than one specimen was measured. N: number of specimens used in the mean (in brackets number of outliers); m: cumulate mass measured. Provenance code: see # in Table 1. Anomalies not included in Table 4 means are listed at the end for each group (name in italics). Pairing notes: (1) DaG 084, 164, 165, 319, 340, 485, 494, 660, 897 (2) FRO 90036-54-168-228-233, 93008, 95028, 01012, 03022.

Meteorite	Group	Log $\chi$	s.d.	N	m (g)	Provenance
LEW 88201	URE	3.89		1	2.8	19
META78008	URE	4.47		1	6	19
Nilpena	URE br	4.06	0.12	3	8.7	8, 21
North Haig	URE br	4.43	0.17	4	15.1	12, 15, 20
Nova 1	URE	4.14	0.04	3	48.9	12, 15, 21
Novo-Urei	URE	4.91	0.11	6	66.1	1, 2, 6, 7, 8, 11
NWA 1464	URE	4.60		1	22.4	31
NWA 1782	URE	4.59	0.02	3	20.4	8
NWA 4742	URE br	4.08		1	32.2	30
NWA 766	URE	4.33	0.03	2	18.2	5, 8
PCA 82506	URE	4.50		1	181	20
QUE 93341	URE	4.10		1	1.8	19
RAS 247	URE	4.39		1	537	23
Reid 016	URE br	4.53		1	18.4	21
RKPA80239	URE	4.58		1	0.2	19
Roosevelt C 27	URE	4.28		1	6	15
Sahara 98505	URE h	4.56	0.03	2	31.6	8
Sahara 02002	URE	4.33		1	28	8
Shiṣhr 007	URE	4.35	0.12	2	2	11
<i>EET 83309-87720</i>	URE br an	3.61	0.04	2	51.4	19
<i>MET 01085</i>	URE an	3.62		1	6.3	19
Acapulco	ACA	5.07		1	14.7	8
ALHA77081-81315-84190	ACA	5.05	0.23	4	9.3	19
Dho 125-290-312	ACA	4.86	0.07	5	325.9	8, 11, 31
Dho 1222	ACA	5.54		1	11.5	8
EET 84302	ACA	5.58		1	6.9	19
FRO 95029	ACA	5.31		1	5.3	3
GRA 98028	ACA	5.00		1	7.4	19
LAP 031323	ACA	5.12		1	1.6	19
MET 01195-98-01232-44	ACA	5.03	0.14	4	115.3	19
Monument Draw	ACA	5.48		1	95	12
NWA 725-1158	ACA	5.71	0.10	4	228	5, 8, 17, 26
RBT 04228	ACA	5.34		1	13.5	19
FRO 93001-95029-03001	ACA/LOD	5.37	0.31	2	3	3
LEW 86220	ACA/LOD	5.74	0.06	2	12.8	20
GRA 95209	LOD	5.75	0.05	3	22.6	19
Lodran	LOD	5.76	0.07	2	33.2	8, 21
NWA 3341	LOD	5.1		1	18.2	30
<i>MAC 88177</i>	LOD	3.94	0.00	2	13.4	19
DaG 565	WIN	4.51	0.07	2	5.3	8
Fortuna	WIN	5.27		1	9.5	31
HaH 193	WIN	4.68		1	22.9	16
Mount Morris	WIN	4.60		1	50	12
NWA 1463	WIN	5.54	0.14	2	15.6	26
Pontlyfni	WIN	5.34	0.05	2	75.8	8, 12
QUE 94535	WIN	4.46		1	6	19
Sahara 02029	WIN	5.21		1	18.5	8
Tierra Blanca	WIN	4.55	0.20	4	27.7	8, 17, 20
Winona	WIN	4.69	0.22	5	232.9	8, 20

Table 2. *Continued.* Decimal  $\log\chi$  (in  $10^{-9}$  m<sup>3</sup>/kg) for achondrites except HEDs, after tentative pairing for desert finds. For ureilites, the anomalous (an), brecciated (br), or unbrecciated and highly shocked (h) characters are indicated. Among SNC meteorites the two magnetic subgroups are separated. Arithmetic mean and standard deviation (s.d., computed using N-1 as normalizer) of  $\log\chi$  are provided when more than one specimen was measured. N: number of specimens used in the mean (in brackets number of outliers); m: cumulate mass measured. Provenance code: see # in Table 1. Anomalies not included in Table 4 means are listed at the end for each group (name in italics). Pairing notes: (1) DaG 084, 164, 165, 319, 340, 485, 494, 660, 897 (2) FRO 90036-54-168-228-233, 93008, 95028, 01012, 03022.

Meteorite	Group	Log $\chi$	s.d.	N	m (g)	Provenance
DaG 896	UNGR	3.53		1	1.8	3
Dho 500	UNGR	4.49		1	23.5	11
Dho 732	UNGR	4.18		1	30.8	11
Divnoe	UNGR	4.93	0.20	2	216.2	11, 26
GRA 06128	UNGR	2.43	0.05	3	138.4	19
NWA 011-2400-4792	UNGR	2.66	0.07	4	95.5	11, 30
NWA 1235	UNGR	5.19		1	2.1	11
NWA 1982	UNGR	5.56		1	24.6	5
NWA 4042	UNGR	5.03		1	1.5	5
RBT 04239	UNGR	4.81		1	2.6	19
Sahara 03500	UNGR	4.22		1	18	8
Tafafasset	UNGR	5.26	0.16	4	11.8	8
Zakłodzie	UNGR	5.16		1	20.6	8

finds (Jull 2006). This trend may also be seen in the high metal content of falls, although it is marginally significant with only 3 falls measured. This hypothesis will have to be further tested using detailed terrestrial age determinations for ureilites.

#### Acapulcoites-Lodranites and Winonaites

Among the Antarctic FRO meteorites we separated two different falls according to Burrioni and Folco (2008). For acapulcoite-lodranites only two falls exist: Acapulco at 5.07 and Lodran at 5.76. One may see a tendency for a larger amount of metal in lodranites than in acapulcoites: mean  $\log\chi$  are  $5.55 \pm 0.30$  and  $5.26 \pm 0.28$ , respectively (counting FRO 93001 and LEW 96220 as lodranite and excluding MAC 88177). However, this difference may not be significant considering that some dispersion is also due to weathering. We prefer instead to use the combined acapulcoite-lodranite mean at  $5.34 \pm 0.30$ . MAC 88177 lodranite, at 3.94, is definitely an outlier in terms of metal content (as described by Takeda et al. 1994).

The  $\log\chi$  value of the only winonaite fall, Pontlyfni, at 5.34 is clearly higher than the mean of all other winonaites,  $4.83 \pm 0.4$ . This is likely due to weathering of metal in finds.

#### Angrites, Aubrites, Brachinites

Angrites (excluding NWA 3164), with a rather well-defined mean  $\log\chi$  at  $2.89 \pm 0.19$ , yield the lowest mean  $\log\chi$  value of all the meteorite groups, though individual aubrites, diogenites and eucrites do show lower  $\log\chi$  values (see section Martian Meteorites). Pyrrhotite (e.g., Kurat et al. 2004), titanomagnetite (e.g., Floss et al. 2003), and metal are reported in angrites. However, the reported composition of

“titanomagnetite” (Table 38 of Mittlefehldt et al. 1998) is  $\text{Ti}_{0.6}\text{Al}_{0.15}\text{Fe}_2\text{M}_{0.25}\text{O}_4$  for Angra dos Reis, M being Mg, Ca, Si, Mn, Cr by order of abundance, and  $\text{Ti}_{0.68}\text{Al}_{0.19}\text{Fe}_{1.73}\text{M}_{0.4}\text{O}_4$  for LEW 86010. These compositions are close to the ulvöspinel end-member ( $\text{Fe} \leq 2$ ) and indicate a paramagnetic state at room temperature. To investigate the relative contribution of pyrrhotite, (titano)-magnetite and metal in the magnetic properties of angrites we performed hysteresis measurements on three angrite samples and compared the shapes of their hysteresis loops with typical ones for metal (Fig. 5), pyrrhotite and magnetite (Rochette et al. 2005). Metal (in multidomain state) is characterized by a curvature up to 0.7 T and very limited hysteresis (very low  $M_{rs}/M_s$  and coercive field  $B_c$ ). The measured angrites clearly have a contribution of magnetite or less likely pyrrhotite (visible by the  $M_{rs}/M_s$  in between 0.11 and 0.26 and  $B_c$  in between 17 and 31 mT) superimposed on the one of metal, as proposed by Weiss et al. (2008). However, the signal of metal may dominate the susceptibility. Therefore, the  $\log\chi$  variation in angrites likely corresponds to variations in the amount of metal with possible contribution from magnetite and pyrrhotite (added onto the baseline paramagnetic susceptibility carried by the silicates and spinels). The “metal-rich” angrite NWA 3164–5167 (paired with NWA 2999: Kuehner et al. 2006) shows a  $\log\chi$  of 4.64. However, its hysteresis points toward magnetite as the major mineral instead of metal. Metal is assumed to have been converted into magnetite by terrestrial weathering (B. Weiss, personal communication). Its metal/magnetite content (about 10 wt%) is two orders of magnitude higher than the metal content in “normal” angrites, making it definitely an anomalous angrite.

Brachinites show much larger mean  $\log\chi$  and dispersion:  $3.75 \pm 0.43$ . EET 99407, at 2.95, could be considered as an

Table 3. Decimal  $\log\chi$  (in  $10^{-9}$  m<sup>3</sup>/kg) for HED achondrites and mesosiderites. The polymict (P) character is indicated. Pairing notes: (1) DaG 276, 380, 391, 411, 480, 567.

Meteorite	Group	Log $\chi$	s.d.	N	m (g)	Provenance
Aioun el Atrouss	DIO P	2.86	0.05	2	40.1	8, 20
Bilanga	DIO	2.80	0.12	4	59.7	5, 8
Dho 700	DIO	3.04	0.02	3	238.6	11
EETA79002	DIO	3.11		1	15.8	20
Ellemeet	DIO	2.71	0.06	2	33	8, 31
Garland	DIO P	3.60	0.15	3	83	8, 20
Ibbenburen	DIO	2.77	0.05	6	37.2	5, 8, 20
Johnston	DIO	3.49	0.23	10	652	2, 3, 7, 8, 17, 21, 32
Manegaon	DIO	2.83		1	1.3	8
MET 00422	DIO	2.46		1	18.3	19
NWA 1239	DIO P	3.20		1	2.2	5
NWA 2515	DIO	3.13	0.02	2	75.9	8
NWA 4272	DIO	3.36		1	56.5	5
Peckelsheim	DIO P	3.03		1	1.8	20
Roda	DIO	2.94	0.09	2	59.7	1, 8
Shakla	DIO	2.95	0.03	4	73.1	1, 6, 8, 11
Tatahouine	DIO	3.15	0.45	10	431.2	3, 7, 8, 11, 18
Y-74013	DIO	3.21	0.25	3	2.8	14
Y-74136	DIO	2.82		1	0.56	14
Nuevo Laredo	EUC	2.96	0.05	3	113.3	8, 20
Palo Blanco	EUC	2.87	0.10	3	29.4	15
Agoult	EUC	2.67	0.08	4	12.2	5, 8, 27
Alby sur Cheran	EUC	2.89		1	10.7	8
ALH 80102	EUC P	2.62	0.04	2	233.2	20
ALHA76005-78165	EUC P	3.31	0.01	2	21.3	20
ALHA81010-12	EUC P	2.85	0.06	2	159.6	20
Bereba	EUC	3.40	0.03	4	54.2	8, 9
Bialystok	EUC P	3.76	0.72	5	207.2	11, 12, 16, 20, 22
Binda	EUC	3.04	0.04	2	195.7	20
Bouvante	EUC	3.21	0.27	4	653.9	8
Brient	EUC P	3.86	0.11	2	192.3	11
Cachari	EUC	2.66	0.03	2	103.1	3, 8
Caldera	EUC	2.70		1	67.7	8
Chervony Kut	EUC	2.71	0.10	3	139	11, 21
DaG 276(1)	EUC P	3.12	0.08	7	175.4	1, 5, 8, 16, 21
DaG 684-945	EUC	2.64	0.07	2	254	3, 5
Dho 7	EUC	2.61		1	17.2	11
Dho 55-275-285-300	EUC P	2.87	0.09	4	191.4	11, 16
Dho 930-1286	EUC	3.12	0.05	2	254	11
EET 83231	EUC P	2.58		1	55.1	20
EET 83234-83283-87531	EUC	2.86	0.10	3	214.6	20
EET 92023	EUC	3.36		1	2.8	19
FRO 97045	EUC P	2.73		1	4.1	3
GRA 98033-98	EUC	2.62	0.02	2	102.5	19
GRV 051523	EUC	2.61		1	0.8	33
HaH 262	EUC	2.79	0.11	2	98.6	5, 8
HaH 059	EUC	3.14		1	17.5	16
Haraiya	EUC	2.75	0.06	3	60.1	12, 21
Ibitira	EUC	2.95	0.05	4	22	8, 11, 18
Igdi	EUC	3.03	0.03	2	23.9	5, 27
Jonzac	EUC	2.68	0.06	4	82.3	1, 7, 8, 10
Juvinas	EUC	2.90	0.17	0	858	1, 9, 10, 11, 17, 18, 32
Lakangaon	EUC	2.83	0.09	2	10.9	8, 20
LEW 85303	EUC	2.81		1	127.4	20
Macibini	EUC P	3.21	0.14	2	19.4	8, 20

Table 3. *Continued.* Decimal  $\log\chi$  (in  $10^{-9}$  m<sup>3</sup>/kg) for HED achondrites and mesosiderites. The polymict (P) character is indicated. Pairing notes: (1) DaG 276, 380, 391, 411, 480, 567.

Meteorite	Group	Log $\chi$	s.d.	N	m (g)	Provenance
Malvern	EUC P	3.49	0.02	4	25.5	8, 12, 20
Medanitos	EUC	2.49		1	6.1	1
Millbillillie	EUC	2.68	0.06	36	585.6	3, 4, 17, 18
Moama	EUC	3.47	0.35	3	33.1	12, 20
Moore County	EUC	2.98	0.05	3	439.5	8, 12, 20
Nagaria	EUC	3.39		1	4.8	12
Nobleborough	EUC P	3.05	0.02	3	20.5	13, 29, 34
NWA 2362	EUC	2.83		1	13.3	21
NWA 3138	EUC	2.61	0.08	2	56.9	21
NWA 999	EUC	2.70		1	12.9	26
NWA 049	EUC P	2.84		1	0.8	12
NWA 1109	EUC P	3.24	0.46	3	13.9	5, 18
NWA 1240	EUC	3.05		1	3.6	5
NWA 1764	EUC	2.66	0.04	3	20	8
NWA 1768-89	EUC	2.90	0.08	2	6.1	8
NWA 2516	EUC	3.23	0.00	2	29.9	8
NWA 47	EUC	2.75		1	4	5
NWA 769	EUC	2.69	0.02	2	18.5	5, 18
Padvarninkai	EUC	2.89	0.20	7	229.9	6, 7, 8, 11, 17
Palo Blanco Creek	EUC	2.89	0.01	2	8.1	11, 17
Pasamonte	EUC P	3.01	0.09	4	141.2	7, 8, 11, 17
PCA 82502-91007	EUC	2.52	0.15	4	285.9	20
Peramio	EUC	2.96	0.17	2	135.6	16, 31
Rancho Blanco	EUC	3.11		1	20.6	29
Serra de Mage	EUC	2.91	0.25	4	287.1	8, 18
Sioux County	EUC	3.16	0.36	5	205.1	7, 8, 20
Smara	EUC P	3.40	0.08	2	100	8, 11
Stannern	EUC	2.78	0.22	14	220.7	1, 6, 8, 10, 11, 17, 18, 22
Sahara 02501	EUC	2.90	0.09	2	3605	5
Talampaya	EUC	2.44	0.02	2	47.8	12, 21
Vetluga	EUC	3.40	0.12	2	9.2	11
Viksdalen	EUC	2.92		1	434.6	22
Y-75011	EUC P	3.08		1	0.77	14
NWA 2247	EUC	3.25	0.02	2	2.9	8
<i>Camel Donga</i>	EUC	4.30	0.19	15	788	3, 8, 17, 21, 22
<i>Pomodзино</i>	EUC	4.08		1	19.6	11
Bholgati	HOW	3.52	0.08	2	14	8, 11
Bununu	HOW	3.54	0.20	3	4.1	8, 20
Chaves	HOW	2.91	0.11	2	82.7	8, 34
DaG 669-881-915-932	HOW	3.08	0.18	6	57.2	3
Dho 18	HOW	3.25		1	7.9	11
Erevan	HOW	3.40		1	27.8	11
Frankfort	HOW	3.45	0.07	2	13.6	8
Hugues 4-5	HOW	3.00	0.04	2	14.4	15, 24
Jodzie	HOW	3.45	0.26	2	6.1	8, 11
Kapoeta	HOW	3.62	0.18	4	43.6	7, 8, 11
Le Teilleul	HOW	3.27	0.01	2	368.4	8
Luotolax	HOW	3.22	0.06	34	47.3	7, 8, 11, 17, 21
Massing	HOW	3.32		1	0.26	12
Melrose B	HOW	3.25		1	6.3	12
Molteno	HOW	3.47	0.06	2	63.8	12
Monticello	HOW	2.72		1	17.6	13
Muckera 002	HOW	3.48		1	20.6	20
Mundrabila 020	HOW	3.19		1	0.9	21
NWA 1281	HOW	3.47		1	13.3	26

Table 3. *Continued.* Decimal  $\log\chi$  (in  $10^{-9}$  m<sup>3</sup>/kg) for HED achondrites and mesosiderites. The polymict (P) character is indicated. Pairing notes: (1) DaG 276, 380, 391, 411, 480, 567.

Meteorite	Group	Log $\chi$	s.d.	N	m (g)	Provenance
NWA 1150	HOW	2.97		1	5.9	5
NWA 1664	HOW	3.52		1	241	16
NWA 1769	HOW	3.40	0.08	2	16.7	8
Old Homestead 001	HOW	3.62		1	39.9	8
Pavlovka	HOW	3.23	0.18	5	192.9	8, 18
Washougal	HOW	3.31		1	16.9	12, 29
Y-7308	HOW	3.30		1	14.2	20
Yurtuk	HOW	2.98	0.10	2	52.6	11, 20
Zmenj	HOW	3.35	0.03	2	21.9	11
<i>Petersburg</i>	HOW	4.26	0.42	7	62.5	1, 2, 8, 9, 22
Barrea	MES	5.70		1	21.9	7
Crab Orchard	MES	5.72		1	110	7
Estherville	MES	5.55	0.05	2	190	7, 32
GRV 020124-0175-1525	MES	5.59	0.03	3	6.9	33
Hainholz	MES	5.69	0.03	2	76.6	7
Morristown	MES	5.66		1	17.7	7
Vaca Muerta	MES	5.66	0.03	2(1)	107.3	5, 7
Veramin	MES	5.82		1	6	32
<i>Bondoc</i>	MES	4.76		1	40.8	7
<i>GRV 050212</i>	MES	5.39		1	12.3	33

outlier, but it has not been excluded from the mean given the small number of meteorites and the large dispersion even among the other brachinites ( $3.85 \pm 0.33$ ). We note that Brachina is very heterogeneous, with a s.d. of 0.42. This spread does not allow us to establish pairing with the four other measured brachinites from southern Australia. We can only say that such pairing is compatible with the log values.

Aubrites appear unique among all meteorite groups for their extreme heterogeneity in metal amount, as testified by a mean of individual standard deviations of 0.39. The largest individual s.d.s. (from 0.5 to 0.7) are found for Bishopville, Bustee, Cumberland Falls, and Mount Egerton. Mount Egerton is an extreme case with  $\log\chi$  ranging from 3.5 to 5.75 on samples in the 15–100 g range. This is clearly due to the generally very coarse grained texture of the aubrites, yielding enstatite crystals or metal nuggets of a few cm in size. Two aubrites, Mayo Belwa and Shallowater, appear homogeneous at the cm scale, as testified by individual s.d. less than 0.1. Despite the measurement of numerous specimens for most aubrites, the mean log for the group, at  $3.79 \pm 0.77$ , still shows a very large scatter. Excluding the two most metal-rich aubrites, Shallowater and Mount Egerton, already recognized as anomalous (Mittlefehldt et al. 1998), plus Queen Alexandra Range (QUE) 97289 and LaPaz Icefield (LAP) 03719, does not reduce dramatically the mean and s.d. of  $3.69 \pm 0.47$ . This indicates a strongly heterogeneous metal distribution not only at a few cm scale, but also at the much larger scale represented by different falls (assuming they come from the same parent body). We note that LAP 03719 shows the lowest  $\log\chi$  value (1.96) of all measured non-lunar meteorites (Rochette et al. 2008).

### Martian Meteorites

Magnetic properties of Martian meteorites have been reviewed at length in Rochette et al. (2001b and 2005), as well as in Van de Moortele et al. (2007) and they will only be summarized here. Whenever possible, we used only large samples, not reported in the previous papers, for the  $\log\chi$  database in order to provide more representative values than those obtained from the subgram samples used in the detailed rock magnetic investigations. Even excluding the metal-rich chassignite NWA 2737 ( $\log\chi = 4.41$ ), Martian meteorites yield a large range of  $\log\chi$  with mean value  $3.18 \pm 0.31$  (on 28 unpaired meteorites). One may distinguish the magnetite-bearing basaltic shergottites (Dhofar 378, Los Angeles), ilherzolitic shergottites and nakhlites, showing a mean at  $3.44 \pm 0.23$ , from the pyrrhotite-bearing basaltic shergottites (plus Chassigny and ALH 84001 pyroxenite) at  $2.97 \pm 0.17$ . In this latter group, the paramagnetic susceptibility dominates. The distinction between the low and high magnetic Martian meteorite groups is grounded in terms of magnetic mineralogy, but their ranges of  $\log\chi$  overlap.

### HED

Once a few metal-rich outliers are excluded, the mean  $\log\chi$  for diogenites, eucrites, and howardites are  $3.02 \pm 0.28$ ,  $2.95 \pm 0.30$ , and  $3.29 \pm 0.23$ , respectively. This indicates that diogenites and eucrites have nearly the same average low metal amount, while howardites are distinctively richer in metal. This may sound surprising as howardites are a mixture of diogenitic and eucritic materials (Mittlefehldt et al. 1998). However, like lunar regolith breccias (Fuller and Cisowski

Table 4. Mean  $\log\chi$  with standard deviation and number of meteorites for the different achondrite groups discussed in the present paper. The number of meteorites, if any, excluded from the mean are reported within brackets (see discussion in the text). The mean of individual s.d. (obtained on several specimens of the same meteorite) and the median of specimen mass are also indicated. The same data for selected chondrite groups (after Rochette et al. 2003 and 2008) is indicated, as well as for examples of terrestrial extrusive rocks (basaltic and rhyolitic flow from the Ethiopian traps after Rochette et al. 1999) and intrusive rocks (granites from Corsica and Sardinia after Gattacceca et al. 2004). In the terrestrial case, N is the number of sites (flow or outcrop), each one consisting of 3 to 9 specimen of about 10 cm<sup>3</sup> each.

Class	$\log\chi$	s.d.	N	Mean s.d.	Median mass (g)
URE unbr	4.39	0.29	47(1)	0.06	
URE br	4.38	0.47	7(1)	0.17	7.2
ACA/LOD	5.34	0.30	17(1)	0.13	6.9
WIN	4.88	0.41	10	0.14	9.4
ANG	2.89	0.19	9(1)	0.10	1.9
AUB	3.79	0.77	16	0.39	10.8
BRA	3.75	0.43	9	0.15	6.4
SNC(high)	3.44	0.23	12(1)	0.08	2.8
SNC(low)	2.97	0.17	16	0.10	4.4
DIO	3.02	0.28	19	0.13	9.6
EUC	2.95	0.30	70(2)	0.11	13.3
HOW	3.29	0.23	28(1)	0.11	8.2
MES	5.67	0.08	8(2)	0.04	19.8
E falls	5.48	0.11	14(1)	0.11	14.3
CO3 falls	4.54	0.20	6	0.06	14.1
CK	4.64	0.14	21(2)	0.06	8.7
R	3.17	0.19	23(3)	0.08	4.2
LL falls	4.11	0.30	43	0.09	8
L falls	4.87	0.10	140	0.06	24
H falls	5.32	0.10	143	0.06	16.3
Ter. extrusives	4.01	0.52	17	0.13	28
Ter. intrusives	3.39	0.61	20	0.17	26

1987; Pieters et al. 2000), howardites may be enriched in metal produced by the regolith-forming processes (space weathering, impact reduction of paramagnetic silicates, and contamination with chondritic metal or magnetite; Hewins [1979]; Zolensky et al. [1996]; Gounelle et al. [2003]). The metal-rich outliers not included in the means are Camel Donga, Petersburg and Pomodzino, with  $\log\chi$  around 4.3. Camel Donga (Palme et al. 1988) and Petersburg (Hewins 1979) have already been recognized as anomalously metal-rich.

Figure 6 shows the frequency histogram of  $\log\chi$  for HEDs and further illustrates the dichotomy between diogenites/eucrites, with a main mode in the 2.7–3 range and howardites with a main mode in the 3.2–3.5 range. A minority of eucrites and diogenites with a “howardite-type” metal enrichment can be defined by a  $\log\chi$  in the 3.3–3.7 range.

These include the diogenites Garland and Johnson, and the eucrites ALH 76005, Bereba, Brient, Malvern, Moama, Nagaria, Smara, and Vetluga (plus the metal rich Camel Donga and Pomodzino with  $\log\chi$  at 4.3). Among these eucrites, Brient, Malvern, and Smara are polymict. The metal content seems to increase marginally with the polymict character: the mean log for polymict eucrites is  $3.03 \pm 0.3$ , compared to  $2.93 \pm 0.3$  for all eucrites.

HEDs have been shown to be closely related to mesosiderites (Mittlefeldt et al. 1998; Greenwood et al. 2006). Therefore we include here some data on mesosiderites (Table 3), although as stony-iron meteorites, they were not subjected to systematic measurements. Terho et al. (1993) reported data on 7 mesosiderites and Lin et al. (2008) on 4 (likely two unpaired); the mean value of 8 (out of 10) meteorites gives the expected high apparent susceptibility with an average value of  $5.67 \pm 0.08$ . This nearly pure metal value (5.74) confirms the interaction hypothesis discussed in section Magnetic Mineralogy of Stony Achondrites. Indeed, it would correspond according to the calibration of Fig.1 to 85% metal, instead of the actual 50%. On the other hand, a 41 g metal-poor sample of Bondoc gave a  $\log\chi$  of 4.76. We also obtained a value of 3.22 on a eucrite-like 50 g fragment of Vaca Muerta. Therefore, one may wonder if some metal-rich HEDs (especially Camel Donga, Petersburg, and Pomodzino) represent a transition toward mesosiderites.

### Ungrouped Achondrites

$\log\chi$  similarities can be used among other criteria to define affinities between unclassified or anomalous achondrites and a given group. NWA 1235 and Zakłodzie ( $\log\chi \approx 5.2$ ), classified as anomalous aubrite or E impact melt (Keil 2007) are clearly richer in metal than the other aubrites. Divnoe and Taffassaset (Table 2) have been recently related to brachinites (Gardner et al. 2007). Again, they are more magnetic than the brachinites (RTB 04239, NWA 1982, and NWA 4042 may also be related to brachinites). In the two cases (aubrite-related and brachinite-related), one may hypothesize that, unlike evolved achondrites like HEDs, Martian meteorites and angrites, the parent body or bodies of the aubrites and brachinites experienced only limited metal/silicate melt segregation in a partially melted chondritic precursor. The range of metal contents observed would reflect the range of partial segregation. The segregation would be minimal in Zakłodzie (versus typical aubrites) and Taffassaset and Divnoe (versus typical brachinites).

Dho 500 (Lorenz et al. 2003) and 732 (Demidova et al. 2004) are orthopyroxene-rich achondrites that show  $\log\chi$  values of 4.5 and 4.2. They are suggested to be related to ureilites or winonaites, the former hypothesis being in agreement with their  $\log\chi$  value.

Among the weakly magnetic ungrouped achondrites,

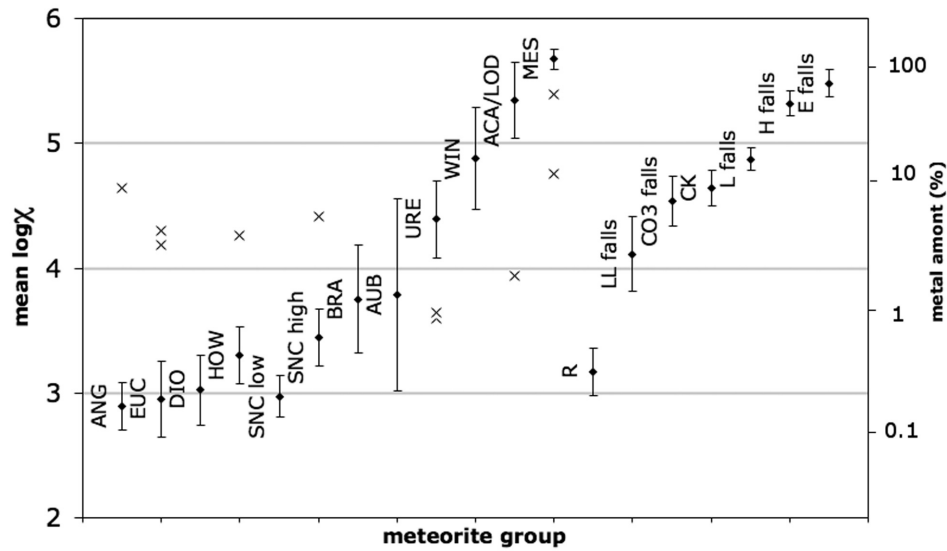


Fig. 2. Mean  $\log\chi$  (in  $10^{-9}$  m<sup>3</sup>/kg) for the different studied achondrite groups (Table 4), compared to selected chondrite groups. Meteorites excluded from the mean appear with crosses. Falls only are used for OC (after Rochette et al. 2003), CO<sub>3</sub> and E (after Rochette et al. 2008). The metal amount (wt%) indicated is a maximum value, assuming non interacting multidomain spheres (see section Magnetic Mineralogy of Stony Achondrites) and not taking into account paramagnetic susceptibility.

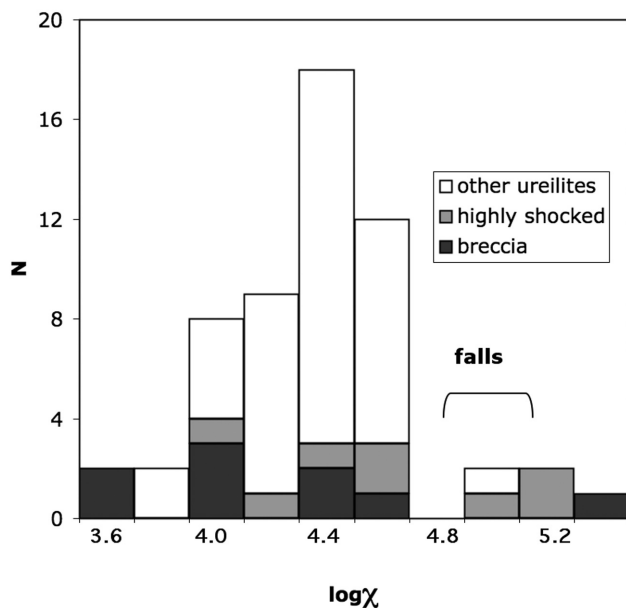


Fig. 3.  $\log\chi$  histogram for ureilites (0.2 increment), separating breccia and highly shocked meteorites.

NWA 011, 2400, and 4792 have indistinguishable  $\log\chi$  value (in the low range of eucrites), supporting their supposed pairing, while GRA 06128 is among the most weakly magnetic achondrites. With a  $\log\chi < 2.5$ , it can be compared only to feldspathic lunar meteorites (Rochette et al. 2008) and to the cumulate eucrite Talampaya. We note that Ibitira, here classified as an eucrite, has recently been demonstrated to be ungrouped (Greenwood et al. 2005). However, its  $\log\chi$  is indistinguishable from the typical values found for eucrites.

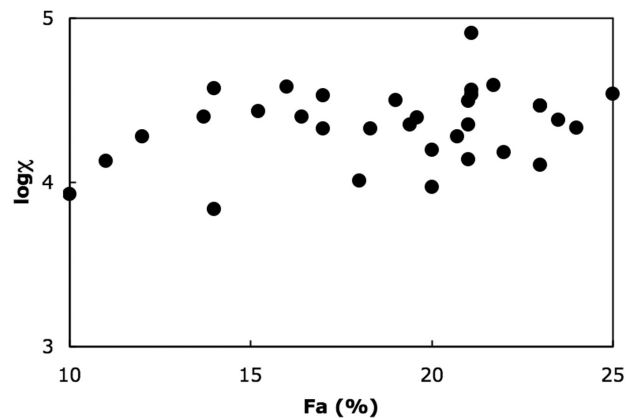


Fig.4.  $\log\chi$  as a function of Fa (mol%) in olivine cores of ureilites (unbrecciated and not highly shocked).

#### THE SATURATION REMANENCE AND GRAIN DENSITY OF ACHONDRITES

The measurement of saturation remanence ( $M_{rs}$ ) needs to be done in a paleomagnetic laboratory, usually requires a small fragment (<5 g), and destroys the paleomagnetic signal. Therefore it was not performed systematically, unlike our susceptibility measurements, but rather as a byproduct of paleomagnetic studies. In Table 5, we have compiled average  $\log M_{rs}$  (in  $10^{-3}$  Am<sup>2</sup>/kg), based on new measurements and on the following references: Brecher et al. (1979), Gattacceca et al. (2004), Nagata (1979), Sugiura (1977), and Weiss et al. (2008). Our data were acquired by saturating samples in a 3 Tesla field and measuring the remanence using a 2G DC SQUID magnetometer. Most of the data correspond to HED

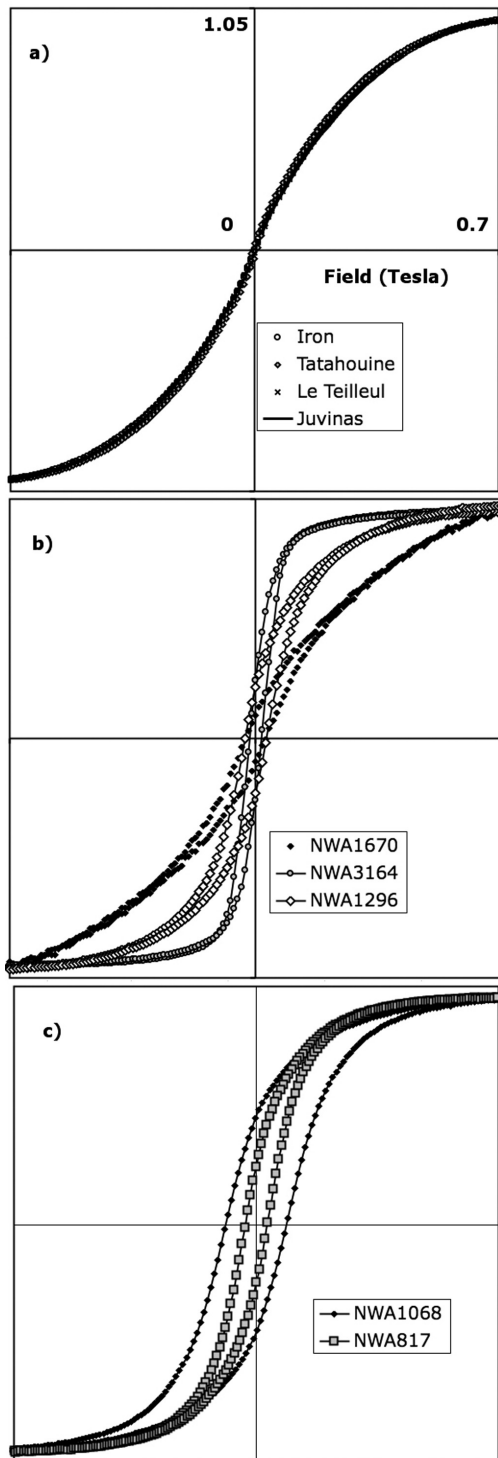


Fig. 5. Hysteresis loops (magnetization normalized to saturation magnetization as a function of field) a) for typical multidomain metal (synthetic sample of Fig. 1, and three HED falls), b) three angrites, c) magnetite- and pyrrhotite-bearing shergottites, after Rochette et al. (2005) and Van de Moortele et al. (2007). All measurements performed using the Micromag VSM in CEREGE, up to 1 T. High field slope has been corrected assuming linearity in between 0.7 and 1 T. Vertical scale is 1.05.

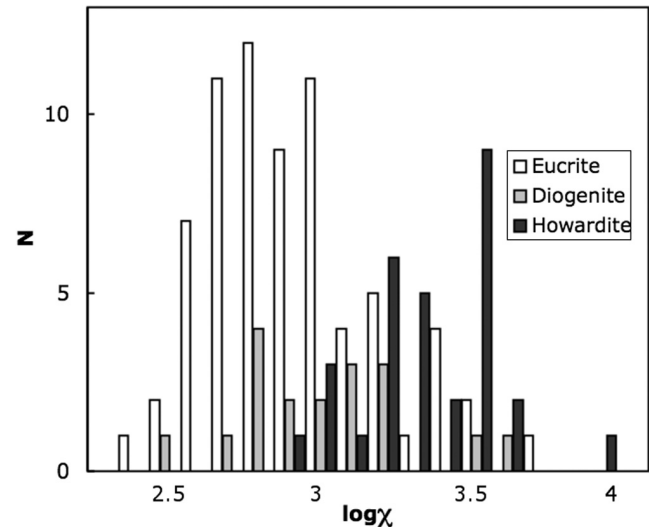


Fig. 6.  $\log \chi$  (values  $< 4$ ) histogram (0.1 increment) for HEDs.

and Martian meteorites (after Rochette et al. [2005], and Van de Moortele et al. [2007]), while scarce data are available for angrites, aubrites, brachinite and ureilites. HED and aubrite  $\log M_{rs}$  data are well below 1, the lowest values being found in eucrites (Fig. 7a). This low remanence in HEDs is at odds with the hypothesis that Vesta has a significant remanence that is able to protect it from the solar wind (Vernazza et al. 2006). This contradiction may be solved by a major contribution of metal-rich HEDs and mesosiderites to the bulk magnetization of Vesta (see below). Higher remanences are found in ureilites (in the 2.3–3.1 range; Fig. 7b), Martian meteorites (mostly in the 1–2.5 range Fig. 7a, except ALH 84001, Chassigny and Sayh al Uhaymir [SaU] 005), the metal rich angrite NWA 3164, and the only brachinite measured. The only mesosiderite fall studied (Estherville, with  $\log M_{rs} = 1.91$ ) as well as iron meteorites ( $\log M_{rs} = 2.38 \pm 0.48$  on 15 samples after Sugiura and Strangway [1987]; Funaki et al. [1988]; Terho et al. [1991]; Funaki and Danon [1998]) yield a low saturation remanence relative to their metal content, as found in E, L, and H chondrites. The other mesosiderite measured, Vaca Muerta, has a higher  $\log M_{rs}$  (2.82), but we suspect it may be linked to weathering. Exceptionally strong remanence can be found in rare tetrataenite-rich samples i.e., Ni-rich irons, with  $\log M_{rs}$  up to 4.6 (Nagata et al. 1987). Angrites (Fig. 7a) are intermediate between metal-bearing HED and magnetite- or pyrrhotite-bearing Martian meteorites, in agreement with their intermediate magnetic mineralogy (see section Angrites, Aubrites, Brachinites). A comparison with chondrites (Fig. 7b, after Rochette et al. [2008]) shows that candidates for significant remanence in the asteroid belt mostly correspond to chondritic or ureilite composition (plus irons and stony-irons). The rough linear correlation between  $M_{rs}$  and  $\chi$  in Fig. 7a shows that both vary with magnetic mineral amount. The slope typical for metal is lower than the slope observed in pyrrhotite- and magnetite-bearing Martian meteorites and chondrites.

Table 5. Mean  $\log M_{rs}$  (in  $10^{-3} \text{ Am}^2/\text{kg}$ ) for achondrites, apart from Martian meteorites (SNC). Reference code is 1: this study; 2: Gattacceca and Rochette (2004); 3: Thero et al. (1993); 4: Brecher et al. (1979); 5: Nagata (1979); 6: Nagata and Funaki (1984); 8: Cisowski (1986); 9: Weiss et al. (2008); 10: Collinson (1991); 11: Brecher and Furhman (1979). Pairing notes: (1) Yamato B-74013-74097-74648-75032, (2) Yamato 74159-74450-75011-790122-790266-791195.

		$\log M_{rs}$	s.d.	ref
Angra dos Reis	ANG	0.06		9
Asuka-881371	ANG	0.71		9
D'Orbigny	ANG	1.03	0.01	9
NWA 1296	ANG	1.22		1
NWA 1670	ANG	1.20		1
NWA 4801	ANG	0.44		9
NWA 3164-5167	ANG	2.11	0.03	1
Bishopville	AUB	0.57		4
Norton County	AUB	0.60	0.43	2, 3
Peña Blanca	AUB	-0.03		2
NWA 4929	BRA	1.88		1
Johnston	DIO	0.32		4
Manegaon	DIO	-0.24	0.13	1
Roda	DIO	0.22	0.46	1, 4
Shakla	DIO	-0.07	0.22	1, 4
Tatahouine	DIO	0.35	0.47	1, 2, 4
Yamato B (1)	DIO	0.58	0.31	5
ALH 76005-77302-78040	EUC	0.35	0.46	6
ALH 81001	EUC	-0.54		8
Bereba	EUC	-0.08		1
Bouvante	EUC	-0.30	0.75	1
DaG 684	EUC	-0.44		2
FRO 97045	EUC	0.15		2
Ibitira	EUC	-0.39	0.15	2, 8
Igdi	EUC	-0.05		1
Juvinas	EUC	0.07	0.16	1, 2, 4
Moore County	EUC	-0.13		8
Nobleborough	EUC	-1.13		4
Pasamonte	EUC	0.12	0.19	1, 4
PCA 82502	EUC	-0.80	0.50	8
Sioux County	EUC	-0.47		4
Stannern	EUC	-0.62	0.10	3, 4
Yamato-74159 (2)	EUC	0.01	0.61	5, 6, 8
Kapoeta	HOW	0.96	0.12	1, 4
Le Teilleul	HOW	0.52	0.27	1, 4
Pavlovka	HOW	0.33	0.29	1, 4
Yamato-7307	HOW	0.43		5
Estherville	MES	1.91	0.21	3, 10
Vaca Muerta	MES	2.82		1
Goalpara	URE	3.00		11
Havero	URE	2.48		11
Kenna	URE	3.05	0.24	11
Novo Urei	URE	2.35		3
NWA 2703	URE	2.79		1
NWA 3140	URE	3.13		1

Consolmagno et al. (2006) showed that fresh ordinary chondrite falls could be unambiguously sorted into H, L, and LL groups on the basis of grain density and magnetic susceptibility. Rochette et al. (2008) showed that density and susceptibility could also differentiate between hydrated and non-hydrated carbonaceous chondrites, though there was a greater spread in the data. Furthermore, the CV and CO

groups tended to plot near the L chondrites, while the enstatite chondrites fell among the H chondrite group.

For achondrites, the separation of classes on the basis of grain density and magnetic susceptibility is not as clear-cut, and there are far fewer samples for which both susceptibility and grain density are available, but certain trends are clear (Fig. 8). The SNC and HED meteorites both lie in the same

general range of susceptibility and grain density, but density and magnetic properties can sort out the various sub-members of each group. Diogenites and eucrites, which have similar low susceptibilities, can be easily separated on the basis of grain density; not surprisingly, howardites overlap both groups. Likewise, the high density of Chassigny easily separates it from the other SNC meteorites in spite of their similar susceptibilities. However, the aubrites plot among the eucrites and howardites, and the ureilites plot with anhydrous carbonaceous chondrites. Overall, in metal-poor achondrites, density is independent of metal amount and reflects mainly the silicate phases (olivine, pyroxene, plagioclase) proportion and composition. The primitive achondrites, as might be expected, overlap with the ordinary chondrite groups in both density and susceptibility albeit with a larger scatter than that seen among the OC.

### DISCUSSION

The use of magnetic susceptibility measurement as a classification tool for achondrites is not as straightforward as in the case of chondrites, which show well-defined values both at the scale of the individual meteorites and for the meteorite group (except CV and CM/C2, see Rochette et al. 2008). On the other hand, the statistical distribution of  $\log\chi$  values for the achondrite groups can be used to discuss their petrogenetic processes. As already pointed out, all achondrites, except unbrecciated ureilites, show significantly larger heterogeneity at the meteorite scale (measured by individual s.d. on  $\log\chi$ ) compared to chondrites (Fig. 9). We infer that this is typical of magmatic processes that allow larger heterogeneities in modal mineralogy at the centimeter scale and above, compared to the accretionary processes in chondrites. To support this interpretation we computed the s.d. on  $\log\chi$  of 10 cm<sup>3</sup> samples of typical terrestrial igneous rocks (Table 4), assuming that the site scale (e.g., a basaltic flow or a granitic outcrop) is equivalent to the meteorite scale. We obtain a mean individual s.d. of 0.13 for the fine-grained extrusive rocks (basalts and ignimbrites) and 0.17 for the coarse-grained intrusive rocks (granites). These values are in the same range as observed for achondrites (Fig. 9). With respect to chondrites, achondrites and terrestrial igneous rocks show the same general trend of increasing individual s.d. with increasing group s.d., but are clearly displaced toward higher individual s.d.. In the case of chondrite groups, outliers are the strongly magnetic ones with individual s.d.  $\geq$  group s.d. due to the effect of demagnetizing field (i.e., sample shape) on the individual dispersion. The mean individual s.d. for unbrecciated ureilites (0.06) is among the lowest of any meteorite group (equaled by only a few chondrite groups). This suggests that the highly homogeneous metal distribution in ureilites (at the meteorite scale) was determined by a post-magmatic petrogenetic process, specific to ureilites. This process may correspond to a late reduction of

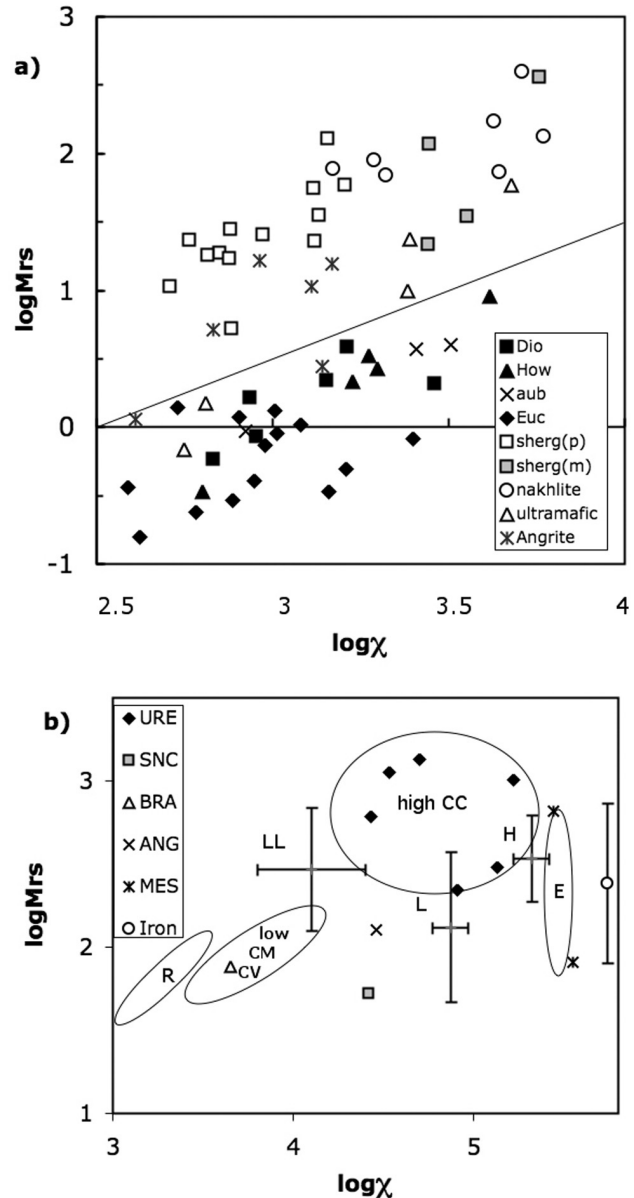


Fig. 7. Log of saturation remanent magnetization  $M_{rs}$  (in  $10^{-3}$  Am<sup>2</sup>/kg) as a function of  $\log a$  for HED (closed symbols), angrites, aubrites, and Martian meteorites (open symbols, separating pyrrhotite- and magnetite-bearing basaltic shergottites, nakhilites, and ultramafic ones), after Rochette et al. (2005) and Van de Moortele et al. (2007). b) For ureilites and other achondrites with  $\log\chi > 3.5$  compared to chondrites ranges or means after Rochette et al. (2003 and 2008).

the olivine grain rims by reaction with carbon (Warren and Huber 2006) during cooling of the ureilites rather than the alternative model of smelting (Goodrich et al. 2007) i.e., simultaneous melting and reduction by the reaction  $MgFeSiO_4 + C \Rightarrow MgSiO_3 + Fe + CO$ .

A common source of  $\log\chi$  dispersion among the various studied groups is the combined effect of terrestrial weathering, brecciation, regolith formation (ureilites and

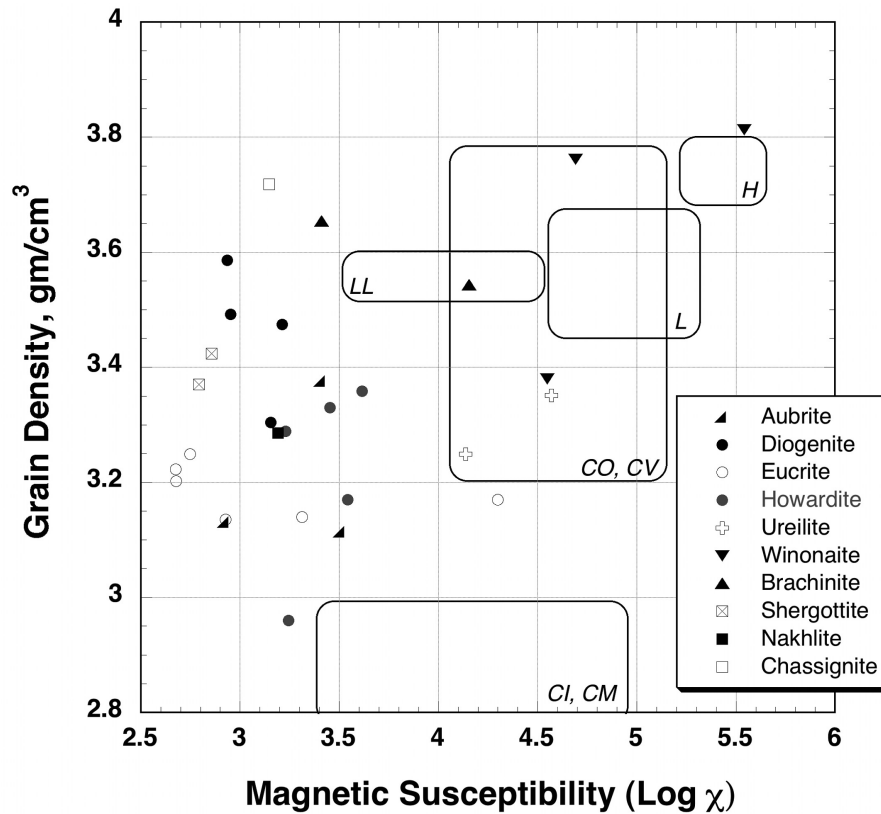


Fig. 8. Grain density (after Britt and Consolmagno [2003], and unpublished data) as a function of  $\log \chi$  for achondrites. Field observed in chondrites are schematized following Consolmagno et al. (2005) and Rochette et al. (2008).

HEDs) and high shock stage up to shock melting (cf. ureilites, NWA 2737 Martian meteorite). Shock melting and/or extreme metamorphism strongly decreases the metal amount by promoting segregation of the metal, as observed in chondrites. DaG 896, classified as an ungrouped achondrite but shown to be an H impact melt (Folco et al. 2004), has a  $\log \chi$  of 3.53 (Table 2), compared to  $5.32 \pm 0.1$  for unmelted H falls. Happy Canyon EL impact melt has a  $\log \chi$  of 4.22 compared to  $5.48 \pm 0.11$  for unmelted E falls (Rochette et al. 2008). Uden LL7 has a  $\log \chi$  of 3.27 compared to a mean for LL falls of  $4.11 \pm 0.3$  (the weakest LL6 being at 3.6). A last explanation that could be put forward for unusual metal enrichment is a contamination by a metal-rich impactor, invoked by Humayun et al. (2007) for angrites.

However, we contend that the phenomena listed above cannot account for the overall metal content dispersion at the meteorite group scale. Figure 10 gives a better visual representation of this dispersion than Fig. 2, by plotting the range of meteorite log values for a given group and its related meteorites. Such dispersion of metal amount, over one or two orders of magnitude, indicates incomplete and heterogeneous metal/silicate segregation. Mechanisms of liquid metal segregation in an asteroid have been modeled by Taylor (1992) and recently reviewed by McCoy et al. (2006). It can proceed in two different ways: porous flow into a solid silicate network, and sinking of metal droplets into a visco-

plastic silicate mush. Porous flow is considered as inefficient unless deformation is active (Rushmer et al. 2005), due to non-wettability of silicates by liquid metal (McCoy et al. 2006). However, this has been challenged by recent experiments (Roberts et al. 2007). In both mechanisms, efficient segregation efficiency depends on gravity and melt duration. Limited melt segregation can be explained either by fast cooling after initial melting (e.g., impact melting) or by near-zero gravity. Near-zero gravity plus melting in a small body is most likely achieved by impact melting, but the fast cooling after impact melting does not fit with the very coarse grain size of the aubrites. Therefore, we are left with the hypothesis of their formation in the core of a sufficiently large body (which would account for initial melting of the core followed by slow cooling). Indeed, in the center of the body gravity is null. Segregation of silicate and metal can be strongly limited in that situation if convection is absent, i.e., if the mechanically liquid zone (>40% partial melting) is limited, and if the melting duration is small (typically of the order of 1 Myr). To quantify these conditions, we computed the settling velocity  $v$  of a metal sphere of radius  $r$  in a silicate liquid core of radius  $R$ , in the case of a Newtonian viscous rheology:  $v = r^2 g \Delta \rho / 9 \eta$ , where  $\Delta \rho$  is the density difference between metal and silicates, and  $\eta$  the silicate liquid viscosity. At a distance  $R$  from the body center, gravity is  $g = G 4 \pi \rho R / 3$ , with  $\rho$  being overall density. Taking  $\rho = 3.5 \cdot 10^3 \text{ kg/m}^3$

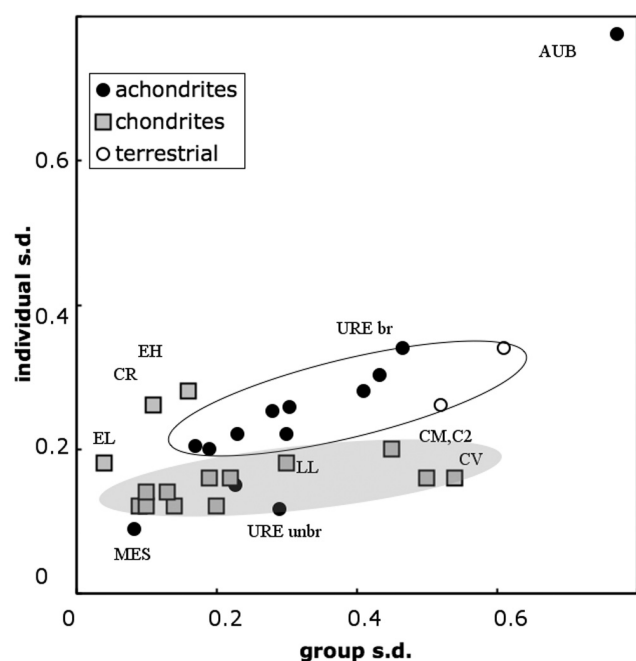


Fig. 9. Mean of  $\log\chi$  individual standard deviation (i.e., at the meteorite scale) versus s.d. of individual means for achondrites groups (see table 4), compared to chondrites (after Rochette et al. 2008) and two sets of terrestrial magmatic rocks (see text and Table 4). White and gray ellipses highlight the main trends for achondrites and chondrites, respectively.

gravity at  $R \leq 10$  km  $g$  is below  $10^{-2}$  N/kg. The viscosities of peridotitic liquids vary according to pressure and temperature (Dingwell et al. 2004; Liebske et al. 2005) but are in the range of  $10^{-1}$  Pa s at temperatures above liquidus. At subliquidus temperatures, higher viscosity, up to  $10^{10}$  Pa s, is expected for chondritic (i.e., more Si rich) melts (Giordano et al. 2006), and in the case where a significant fraction of suspended crystals is present (Bouhifd et al. 2004). The minimum viscosity of  $10^{-1}$  Pa s gives a velocity  $v \leq 3 \times 10^7$  m/Myr for  $r = 100$   $\mu$ m, (using  $\Delta\rho = 4 \times 10^3$  kg/m<sup>3</sup>), i.e., very efficient segregation even for small metal droplets. However, a 1 mm threshold for efficient segregation can be obtained for a viscosity of  $10^5$  Pa s, more plausible under these particular conditions for partial melting (lower temperature, presence of solid phases and Si enrichment). For a viscosity of  $10^5$  Pa s, velocities for  $r = 100$   $\mu$ m and 1 cm are less than 30 m/Myr and 300 km/Myr, respectively. This partial melting case is exemplified by the acapulcoite-lodranite parent body (McCoy et al. 1997; Folco et al. 2006). In that case, small grains may not segregate at all on the 1 Myr time scale into a core with a radius on the order of ten km. Only large blobs will settle and grow by coalescence of small metal droplets, leaving behind them a metal-depleted wake. An alternative model, discussed in Roberts et al. (2007), is based on liquid metal (plus sulfide) percolating through a solid silicate matrix of given permeability. Roberts et al. (2007), using experimentally determined permeabilities for a partially molten metal-

sulfide-silicate mixture (with 10% volume metal-sulfide liquid), computed metal melt migration velocities of 15 km/Myr at  $R = 100$  km, and thus  $\leq 1.5$  km/Myr at  $R \leq 10$  km. Their model also predicts that segregation will not be complete for  $R \leq 10$  km if partial melting lasts just a few Myr.

In our low gravity hypothesis, one would depict primitive achondrites (acapulcoite/lodranites and winonaites) as partially molten cores of moderate-size bodies with very little metal segregation, surrounded by an outer shell consisting of unmelted chondritic material. This situation is well exemplified in the acapulcoite-lodranite parent body, where rocks that experienced a large range of degrees of partial melting (up to more than 35%: McCoy et al. 1997; Folco et al. 2006) have overlapping  $\log\chi$  values. Aubrites and brachinites would follow the same scheme but in a slightly larger body, allowing partial and variable segregation (according to size of the sinking metal blobs). HEDs, angrites, and Martian meteorites are clearly at the other end of the process, being the outer silicate layer of large completely molten and segregated bodies. Still, segregation may not be perfect in the HEDs and angrites as demonstrated by the occurrence of metal-rich meteorites in these groups. The present overall scheme leaves a pending problem for the most primitive achondrites: why was basaltic melt segregation much more efficient than metallic melt segregation when the density difference (with the unmelted material) should favor the opposite (see Mittlefehldt et al. 1997 and McCoy et al. 2006)? It may be due to the lower melting temperature of the basaltic eutectic than that of the metal, giving a much longer time for basaltic melt segregation, or it may involve a process with vapor generation, and/or impact-induced escape of the lighter melt (Wilson and Keil 1991).

## CONCLUSIONS

The measurement of magnetic properties, particularly magnetic susceptibility (expressed as  $\log\chi$  with  $\chi$  in  $10^{-9}$  m<sup>3</sup>/kg), provides a fast and fully non-destructive technique to quantify the modal composition of meteorites in terms of ferromagnetic iron minerals (mainly metal and magnetite, with accessory pyrrhotite, schreibersite, and cohenite). For chondrites, it has proved very useful as a classification tool and to identify anomalous samples (misclassified, mislabeled, etc.), thanks to the restricted range of  $\log\chi$  of each chondrite group, except for the CM/C2 and CV groups. For achondrites, the classification ability is less effective as a rather large dispersion of susceptibility values is observed in a given class, both among multiple specimens of the same meteorite (except for ureilites) and among different meteorites. Moreover, most classes exhibit metal-rich outliers (e.g., NWA 2737 for Martian meteorites, Camel Donga and Pomozdino for eucrites, Petersburg for howardites, NWA 3164 for angrites) or metal-poor outliers (e.g., MAC 88177 for lodranites) with respect to the mean. This heterogeneity in

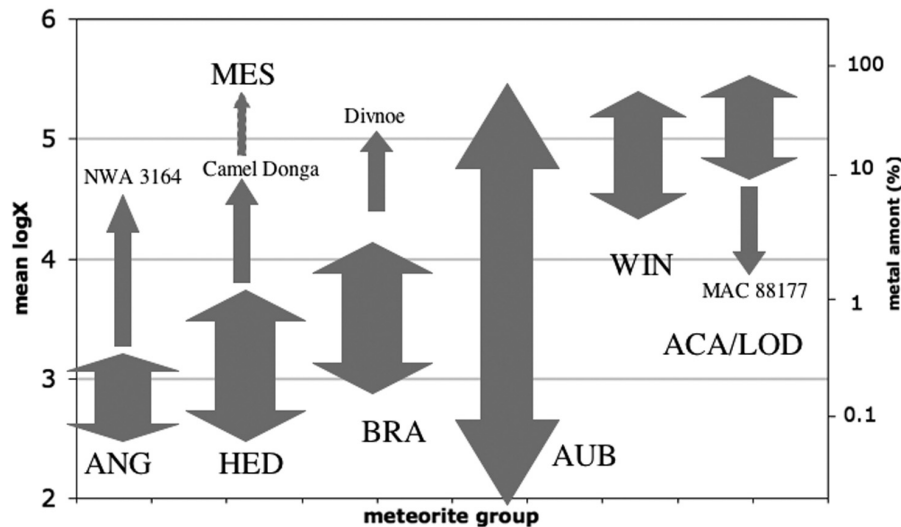


Fig. 10. Range of  $\log\chi$  values observed for the various achondrite groups (except ureilite and Martian meteorites). Main population spread is shown with a thick arrow while outliers or related meteorites (see text) are connected to the main arrow with a thinner one.

metal abundance is typical of magmatic processes (compared to accretionary processes shown to generate high homogeneity in the chondrites). We propose that metal-rich stony achondrites indicate a low gravity origin that impeded efficient core segregation. Such a situation can be encountered in small sized molten cores (of the order of 10 km) surrounded by chondritic shells. Therefore, at least the aubrite, brachinite, winonaite, and acapulcoite-lodranite groups could have their chondritic and eventually transitional counterparts in the meteorite collection. For aubrites, this may correspond to E chondrites and meteorites like Zakłodzie or Itqy. For brachinites, it would be a C chondrite group like CR, with Tafassasset and Divnoe representing the intermediate case. Finally the Acapulco-Lodranite group could be related to the CH chondrite group. Angrites and HEDs would correspond to larger bodies but these still require an imperfect segregation setting. The metal distribution in ureilites is the result of a completely different process characterized by extreme homogeneity. Post solidification olivine rim reduction is the best candidate for such a process. Saturation remanence of HEDs and aubrites is quite weak, and among the stony meteorites, only Martian meteorites and ureilites can generate significant remanent magnetization at the parent body scale.

**Acknowledgments**—The quality of the manuscript was greatly improved by the editing and comments of A. J. Brearley, B. Weiss, and two anonymous reviewers. We are indebted (among others) to R. Bartoschewitz, F. Beroud, J. Boesenberg, F. Brandstaetter, P. Davidson, D. Ebel, C. A. Francis, M. Franco, N. Hiller, R. Hines, P. Gillet, A. Greshake, A. Jambon, B. Kratochvil, Y. Lin, A. Martaus, K. McBride, T. McCoy, G. Motuza, MJ Muñoz-Espadas, M. Nazarov, H. Newsom, J. O. Nyström, M. L. Osete, H.

Pärnaste, J. Plado, B. Poshkiene, G. Raade, K. Righter, A. Rubin, E. Rudnickaite, S. Russell, B. Sanchez, C. Satterwhite, R. Scorzelli, R. Serra, A. Skripnik, J. Szubiakowski, L. Touret, M. Wadwha, J. T. Wasson, B. Weiss, L. Welzenbach, B. Zanda, and M. E. Zucolotto for giving access to their collections and database or for loaning samples and for their help during measurements. This work was supported by the PNP INSU/CNES program and the ANR-05-JCJC-0133-01project.

*Editorial Handling*—Dr. Adrian Brearley

## REFERENCES

- Bouhfid M. A., Richet P., Besson P., Roskosz M., and Ingrin J. 2004. Redox state, microstructure and viscosity of a partially crystallized basalt melt. *Earth and Planetary Science Letters* 218:31–44.
- Brecher A. and Fuhman M. 1979. The magnetic effects of brecciation and shock in meteorites: II. The ureilites and evidence for strong nebula magnetic fields. *The Moon and the Planets* 20:251–263.
- Brecher A., Fuhman M., and Stein J. 1979. The magnetic effects of brecciation and shock in meteorites: III. The achondrites. *The Moon and the Planets* 20:265–279.
- Britt D. T. and Consolmagno G. J. 2003. Stony meteorite porosities and densities: A review of the data through 2001. *Meteoritics & Planetary Science* 38:1161–1180.
- Burroni and Folco L. 2008. Frontier Mountain meteorite specimens of the acapulcoite-lodranite clan: Petrography, pairing and parent-rock lithology of an unusual intrusive rock. *Meteoritics & Planetary Science* 43:1–14.
- Carmichael R. S. 1989. *Practical handbook of physical properties of rocks and minerals*. Boca Raton, FL: CRC Press. 741 p.
- Chevrier V., Mathé P. E., Rochette P., Grauby O., Bourrié G., and Trolard F. 2006. Iron weathering products in a  $\text{CO}_2 + (\text{H}_2\text{O}$  or  $\text{H}_2\text{O}_2)$  atmosphere: Implications for Mars surface. *Geochimica et Cosmochimica Acta* 70:4295–4317.

- Cisowski S. M. 1986. Magnetic study on Shergotty and other SNC meteorites. *Geochimica et Cosmochimica Acta* 50:1043–1048.
- Cisowski S. M. 1991. Remanent magnetic properties of unbrecciated eucrites. *Earth and Planetary Science Letters* 107:173–181.
- Coey J. M. D., Roux-Buisson H., and Brussetti R. 1976. The electronic phase transitions in FeS and NiS. In *Metal-non metal transitions in transition metal compounds*. London: Taylor and Francis.
- Collinson D. W. 1991. Magnetic properties of the Estherville mesosiderite. *Meteoritics* 26:1–10.
- Collinson D. W. 1986. Magnetic properties of Antarctic shergottite meteorites EETA79001 and ALHA77005: Possible relevance to a Martian magnetic field. *Earth and Planetary Science Letters* 77:159–164.
- Collinson D. W. 1997. Magnetic properties of Martian meteorites. *Meteoritics & Planetary Science* 32:803–811.
- Collinson D. W. and Morden S. J. 1994. Magnetic properties of howardite, eucrite and diogenite (HED) meteorite: Ancient magnetizing fields and meteorite evolution. *Earth and Planetary Science Letters* 126:421–434.
- Consolmagno G. J., Macke R. J., Rochette P., Britt D. T., and Gattacceca J. 2006. Density, magnetic susceptibility, and the characterization of ordinary chondrite falls and showers. *Meteoritics and Planetary Science* 41:331–342.
- Dekkers M. J. 1988. Magnetic properties of natural pyrrhotite part I: Behaviour of initial susceptibility and saturation magnetization related rock magnetic parameters in a grain size dependent framework. *Physics of the Earth and Planetary Interiors* 52:376–393.
- Demidova S. I., Nazarov M. A., Kurat G., Brandstätter F., Ntaflos T., Clayton R. N., and Mayeda T. K. 2004. Dhofar 732: A Mg-rich orthopyroxenitic achondrite (abstract #1266). 35th Lunar and Planetary Science Conference. CD-ROM.
- Dingwell D. B., Courtial P., Giordano D., and Nichols A. R. L. 2004. Viscosity of peridotite liquid. *Earth and Planetary Science Letters* 226:127–138.
- Floss C., Crozaz G., McKay G., Mikouchi T., and Killgore M. 2003. Petrogenesis of angrites. *Geochimica et Cosmochimica Acta* 67:4775–4789.
- Folco L., Bland P. A., D’Orazio M., Franchi I. A., Kelley S. P., and Rocchi S. 2004. Extensive impact melting on the H-chondrite parent asteroid during the cataclysmic bombardment of the early solar system: Evidence from the achondritic meteorite Dar al Gani 896. *Geochimica et Cosmochimica Acta* 68:2379–2397.
- Folco L., Rochette P., Gattacceca J., and Perchiazzi N. 2006. In situ identification, pairing and classification of meteorites from Antarctica by magnetic methods. *Meteoritics & Planetary Science* 41:343–353.
- Folco L., D’Orazio M., and Burrioni A. 2006. Frontier Mountain 93001: A coarse-grained, enstatite-augite-oligoclase-rich, igneous rock from the acapulcoite-lodranite parent asteroid. *Meteoritics and Planetary Science* 41:1183–1198.
- Funaki M., Taguchi I., Danon J., Nagata T., and Kondo Y. 1988. Magnetic and metallographical studies of the Bocaiuva iron meteorite. *Proceedings of the NIPR Symposium on Antarctic Meteorites* 1:231–246.
- Funaki M. and Danon J. 1998. Characteristics of natural remanent magnetization of Nova Petropolis iron meteorite. *Antarctic Meteorite Research* 11:189–201.
- Fuller M. and Cisowski S. M. 1987. Lunar paleomagnetism. In *Geomagnetism*, vol. 2, edited by Jacobs J. A. London: Academic Press. pp. 307–455.
- Gardner K. G., Lauretta D. S., and Killgore M. 2007. Petrology of ungrouped achondrites RBT 04239 and Tafassasset: A comparison to Divnoe and the brachinites (abstract #2086). 37th Lunar and Planetary Science Conference. CD-ROM.
- Gattacceca J. and Rochette P. 2004. Toward a robust paleointensity estimate for meteorites. *Earth and Planetary Science Letters* 227:377–393.
- Gattacceca J., Eisenlohr P., and Rochette P. 2004a. Calibration of in situ magnetic susceptibility measurements. *Geophysical Journal International* 158:42–49.
- Gattacceca J., Orsini J. -B., Henry B., Rochette P., Rossi P., and Cherchi G. 2004b. Late-Hercynian tectonic environment revealed by anisotropy of magnetic susceptibility of Hercynian granitoids from southern Corsica and northern Sardinia. *Journal of the Geological Society* 161:277–289.
- Gattacceca J., Rochette P., Denise M., Consolmagno G., and Folco L. 2005. An impact origin for the foliation of ordinary chondrites. *Earth and Planetary Science Letters* 234:351–368.
- Gattacceca J., Rochette P., Gounelle M., and Van Ginneken M. 2008. Magnetic anisotropy of HED and Martian meteorites and implications for the crust of Vesta and Mars. *Earth and Planetary Science Letters* 270:280–289.
- Goodrich C. A. 1992. Ureilites: A critical review. *Meteoritics* 27:327–352.
- Goodrich C. A., Van Orman J. A., and Wilson L. 2007. Fractional melting and smelting on the ureilite parent body. *Geochimica et Cosmochimica Acta* 71:2876–2895.
- Giordano D., Mangiacapra A., Potuzak M., Russel J. K., Romano C., Dingwell D. B., and Di Muro A. 2006. An expanded non-Arrhenian model for silicate melt viscosity: A treatment for metaluminous, peraluminous and peralkaline liquids. *Chemical Geology* 229:42–56.
- Gounelle M., Zolensky M. E., Liou J. C., Bland P. A., and Alard O. 2003. Mineralogy of carbonaceous microclasts in howardites: Identification of C2 fossil micrometeorites. *Geochimica et Cosmochimica Acta* 67:507–527.
- Grady M. 2000. *Catalogue of meteorites*, 5th ed. Cambridge: Cambridge University Press. 689 p.
- Greenwood R., Franchi I., Jambon A., and Buchanan C. 2005. Widespread magma oceans on asteroidal bodies in the early solar system. *Nature* 435:916–918.
- Greenwood R., Franchi I., Jambon A., Barrat J. A., and Burbine T. H. 2006. Oxygen isotope variation in stony iron meteorites. *Science* 313:1763–1765.
- Herrin J. S., Mittlefehldt D. W., Downes H., and Humayun M. 2007. Diverse metals and sulfides in polynict ureilites EET 83309 and EET 87720 (abstract#2404). 38th Lunar and Planetary Science Conference. CD-ROM.
- Hewins R. H. 1979. The composition and origin of metal in howardites. *Geochemica et Cosmochemica Acta* 43:1663–1673.
- Hoffmann V., Funaki M., Torii M., Kurihara T., and Mikouchi T. 2008. Magnetic signature of Iherzolitic shergottites ALH 77005 and Yamato-000097: Brown color olivines and detection of Fe metal particles by magnetotactic bacteria (abstract#1703). 39th Lunar and Planetary Science Conference. CD-ROM.
- Humayun M., Irving A. J., and Kuehner S. M. 2007. Siderophile elements in metal from metal-rich angrite NWA 2999 (abstract#1221). 38th Lunar and Planetary Science Conference. CD-ROM.
- Jarosewich E. 1990. Chemical analysis of meteorites: Compilation of stony and iron meteorite analyses. *Meteoritics* 25:323–337.
- Jull A. J. T. 2006. Terrestrial ages of meteorites. In *Meteorites and the early solar system II*, edited by Lauretta D. S. and McSween H. Y. Jr. Tucson, AZ: The University of Arizona Press. pp. 889–905.

- Keil K. 2007. Occurrence and origin of keilite, (Fe > 0.5, Mg < 0.5)S, in enstatite chondrite impact-melt rocks and impact-melt breccias. *Chemie der Erde* 67:37–54.
- Keil K., Berkley J. L., and Fuchs L. H. 1982. Suessite, Fe<sub>3</sub>Si: A new mineral in the North Haig ureilite. *American Mineralogist* 67:126–131.
- Kohout T., Jackson M., Kosterov A., Kletetschka G., Lehtinen M., and Pesonen L. J. 2007. Low-temperature magnetic properties of the Neuschwanstein EL6 meteorite. *Earth and Planetary Science Letters* 261:143–151.
- Kohout T., Kletetschka G., Elbra T., Adachi T., Mikula V., Pesonen L. J., Schnabl P., and Slechta S. 2008. Physical properties of meteorites—Applications in space missions to asteroids. *Meteoritics & Planetary Science* 43:1009–1020.
- Kuehner S. M., Irving A. J., Bunch T. E., Wittke J. H., Hupé G. M., and Hupé A. C. 2006. Coronas and symplectites in plutonic angrite NWA 2999 and implications for Mercury as the angrite parent body (abstract #1344). 37th Lunar and Planetary Science Conference. CD-ROM.
- Kurat G., Varela M. E., Brandstätter F., Weckwerth G., Clayton R. N., Weber H. W., Schultz L., Wasch E., and Nazarov M. A. 2004. D'Orbigny: A non-igneous angritic achondrite? *Geochimica et Cosmochimica Acta* 68:1901–1921.
- Latham A. G., Harding K. L., Lapointe P., Morris W. A., and Balch S. J. 1989. On the log normal distribution of oxides in rocks, using magnetic susceptibility as a proxy for oxide mineral concentration. *Geophysical Journal International* 96:179–184.
- Lecoanet H., Leveque F., and Segura S. 1999. Magnetic susceptibility in environmental application: Comparison of field probes. *Physics of the Earth and Planetary Interiors* 115:191–204.
- Liebske C., Schmickler B., Terasaki H., Poe B. T., Suzuki A., Funakoshi K., Ando R., and Rubie D. C. 2005. Viscosity of peridotite liquid up to 13 GPa: Implications for magma ocean viscosities. *Earth and Planetary Science Letters* 240:589–604.
- Lin Y., Luo H., Hu S., Feng L., Liu T., and Miao B. 2008. Magnetic susceptibility of Grove Mountains meteorites (abstract #4011). *Meteoritics & Planetary Science* 43:A185.
- Lorenz C. A., Ivanova M. A., Nazarov M. A., Mayeda T. K., and Clayton R. N. 2003. A new primitive ungrouped achondrite, Dhofar 500: Links to winonaite and silicate inclusions from IAB and IIICD irons (abstract #5045). *Meteoritics & Planetary Science* 38:A30.
- McCoy T. J., Keil K., Muenow D. W., and Wilson L. 1997. Partial melting and melt migration in the acapulcoite-lodranite parent body. *Geochimica et Cosmochimica Acta* 61:639–650.
- McCoy T. J., Mittlefehldt D. W., and Wilson L. 2006. Asteroid differentiation. In *Meteorites and the early solar system II*, edited by Lauretta D. S. and McSween H. Y. Jr. Tucson, AZ: The University of Arizona Press. pp. 733–745.
- Mittlefehldt D. W., McCoy T. J., Goodrich C. A., and Kracher A. 1998. Non-chondritic meteorites from asteroidal bodies. In *Planetary materials*, edited by Papke J. J. Reviews in Mineralogy and Geochemistry, vol. 36. Chapter 3.
- Morden S. J. 1992. A magnetic study of the Millbillillie (eucrite) achondrite: Evidence for a dynamo-type magnetizing field. *Meteoritics* 27:560–567.
- Nagata T. 1979. Meteorite magnetism and the early solar system magnetic field. *Physics of the Earth and Planetary Interiors* 20:324–341.
- Nagata T. and Funaki M. 1984. Notes on magnetic properties of Antarctic polymict eucrites. *Memoirs of the National Institute for Polar Research* 35:319–326.
- Nagata T. and Funaki M. 1986. Magnetic properties of Yamato-791197 in comparison with those of lunar highland anorthositic breccias. *Memoirs of the National Institute for Polar Research* 41:152–164.
- Nagata T., Danon J., and Funaki M. 1987. Magnetic properties of Ni-rich iron meteorites. *Memoirs of the National Institute for Polar Research* 46:263–282.
- Palme H., Wlotzka F., Spettel B., Dreibus G., and Weber H. 1988. Camel Donga: A eucrite with high metal content. *Meteoritics* 23:49–57.
- Pesonen L. J., Terho M., and Kukkonen I. 1993. Physical properties of 368 meteorites. Implications for meteorite magnetism and planetary geophysics. *Proceedings of the NIPR Symposium on Antarctic Meteorites* 6:401–406.
- Pieters C. M., Taylor L. A., Noble S. K., Keller L. P., Hapke B., Morris R. V., Allen C. C., McKay D. S., and Wentworth S. 2000. Space weathering on airless bodies: Resolving a mystery with lunar samples. *Meteoritics & Planetary Science* 35:1101–1107.
- Roberts J. J., Kinney J. H., Siebert J., and Ryerson F. J. 2007. Fe-Ni-S melt permeability in olivine: Implications for planetary core formation. *Geophysical Research Letters* 34:L14306, doi: 10.1029/2007GL030497.
- Rochette P. 1987. Magnetic susceptibility of the rock matrix related to magnetic fabric studies. *Journal of Structural Geology* 9:1015–1020.
- Rochette P., Aubourg C., and Perrin M. 1999. Is this magnetic fabric normal? A review and case studies in volcanic formations. *Tectonophysics* 307:219–234.
- Rochette P., Sagnotti L., Consolmagno G., Folco L., Maras A., Panzarino F., Pesonen L., Serra R., and Terho M. 2001a. A magnetic susceptibility database for stony meteorites. *Quaderni di Geofisica* 18. 30 p.
- Rochette P., Lorand J. P., Fillion G., and Sautter V. 2001b. Pyrrhotite and the remanent magnetization of SNC meteorites: A changing perspective on Martian magnetism. *Earth and Planetary Science Letters* 190:1–12.
- Rochette P., Gattacceca J., Menvielle P., Eisenlohr P., and Chevrier V. 2004. Interest and design of magnetic properties measurements on planetary and asteroidal landers. *Planetary and Space Science* 52:987–995.
- Rochette P., Sagnotti L., Bourot-Denise M., Consolmagno G., Folco L., Gattacceca J., Osete M. L., and Pesonen L. 2003. Magnetic classification of stony meteorites: 1. Ordinary chondrites. *Meteoritics & Planetary Science* 38:251–268.
- Rochette P., Gattacceca J., Chevrier V., Hoffmann V., Lorand J. P., Funaki M., and Hochleitner R. 2005. Matching Martian crustal magnetization and meteorite magnetic properties. *Meteoritics & Planetary Science* 40:529–540.
- Rochette P., Gattacceca J., Bonal L., Bourot-Denise M., Chevrier V., Clerc J. P., Consolmagno G., Folco L., Gounelle M., Kohout T., Pesonen L., Quirico E., Sagnotti L., and Skripnik A. 2008. Magnetic classification of stony meteorites: 2. Non-ordinary chondrites. *Meteoritics & Planetary Science* 43:959–980.
- Rochette P., Gattacceca J., Ivanov A., Nazarov M., and Bezaeva N. 2008. Magnetic properties of lunar materials: Comparison between meteorites and sample return (abstract). *Meteoritics & Planetary Science* 43:A133.
- Rubin A. E. 1997. Mineralogy of meteorite groups—An update. *Meteoritics & Planetary Science* 32:733–734.
- Rushmer T., Petford N., Humayun M., and Campbell A. J. 2005. Fe-liquid segregation in deforming planetesimals: Coupling core-forming compositions with transport phenomena. *Earth and Planetary Science Letters* 239:185–202.
- Sagnotti L., Rochette P., Jackson M., Vadeboin F., Dinares-Turrel J., Winkler A., and MAGNET Science Team. 2003. Inter-laboratory calibration of low field and anhysteretic susceptibility

- measurements. *Physics of the Earth and Planetary Interiors* 138: 25–38.
- Smith D. L., Ernst R. E., Samson C., and Herd R. 2006. Stony meteorite characterization by non-destructive measurement of magnetic properties. *Meteoritics & Planetary Science* 41:355–373.
- Sugiura N. 1977. Magnetic properties and remanent magnetization of stony meteorites. *Journal of Geomagnetism and Geoelectricity* 29:519–539.
- Sugiura N. and Strangway D. W. 1987. Magnetic studies of meteorites. In *Meteorites and the early solar system*, edited by Kerridge J. F. and Matthews M. S. Tucson, AZ: The University of Arizona Press. pp. 595–615.
- Takeda H., Mori H., Hiroi T., and Saito J. 1994. Mineralogy of new Antarctic achondrites with affinity to Lodran and a model of their evolution in an asteroid. *Meteoritics* 29:830–842.
- Taylor G. J. 1992. Core formation in asteroids. *Journal of Geophysical Research* 97:14,717–14,726.
- Terho M., Pesonen L. J., and Kukkonen I. T. 1991. The petrophysical classification of meteorites: New results. Geological Survey of Finland Report Q29.1/91/1.
- Terho M., Pesonen L. J., Kukkonen I. T., and Bukovanska M. 1993. The petrophysical classification of meteorites. *Studia Geophysica et Geodetica* 37:65–82.
- Van de Moortèle B., Reynard B., Rochette P., Jackson M., Beck P., Gillet P., McMillan P. F., and McCammon C. A. 2007. Shock-induced metallic iron nanoparticles in olivine-rich Martian meteorites. *Earth and Planetary Science Letters* 262:37–49.
- Warren P. H. and Huber H. 2006. Ureilite petrogenesis: A limited role for smelting during anatexis and catastrophic disruption. *Meteoritics & Planetary Science* 41:835–849.
- Weiss B. P., Lima E. A., and Zucolotto M. E. 2008. Magnetism of the angrite parent body (abstract #2143). 39th Lunar and Planetary Science Conference. CD-ROM.
- Welten K. C., Nishiizumi K., Caffee M. W., and Hillegonds D. J. 2006. Cosmogenic radionuclides in ureilites from Frontier Mountain, Antarctica: Evidence for a polymict breccia (abstract #2391). 37th Lunar and Planetary Science Conference. CD-ROM.
- Wilson K. and Keil K. 1991. Consequences of explosive eruptions on small solar system bodies—The case of the missing basalts on the aubrite parent body. *Earth and Planetary Science Letters* 104:505–512.
- Zolensky M. E., Weisberg M. K., Buchanan P. C., and Mittlefehldt D. W. 1996. Mineralogy of carbonaceous chondrite clasts in HED achondrites and the Moon. *Meteoritics & Planetary Science* 31:518–537.
-